Potentiomics:

Observations of *In Situ* and *In Vitro* Microbial Metabolic Activity Using Type IV Non-Selective Biofilm Membrane Potentiometric Sensors in Real-Time Applications.

by

Evan D. Taylor

A Thesis Presented in Partial Fulfillment
of the Requirements for the Degree
Master of Science

Approved April 2022 by the
Graduate Supervisory Committee:

Taylor Weiss, Chair
Treavor Boyer
Al Brown

ARIZONA STATE UNIVERSITY

May 2022

ABSTRACT

Potentiometric instrumentation technologies are widely used across many disciplines of science and engineering providing the ability to measure changes to specific environmental variables through various types of sensor electrodes and selective membranes. However, types I, II, and III potentiometric sensor electrodes are limited by biofouling activity, membrane maintenance, grounding sensitivity, thermodynamic variables, and electromagnetic interference. Further, algorithms embedded into instrumentation hardware have impeded the usefulness of such measurements outside of highly controlled environments. Reliability of accurate measurement using these types of senor electrodes is limited to industrial and lab applications in chemistry and nominally active biological environments. Novel innovations in using exotic materials have improved the usefulness of Type II (e.g. tantalum-rubidium-doped titanium) and Type III (e.g. Nafion™ membranes) sensor electrodes, but those sensors are still limited to measuring a single selective parameter. This scope of work investigates utilizing a novel non-selective membrane, or naturally occurring biofilm membrane, as the active sensing surface of a graphite electrode as a new Type IV potentiometric sensor electrode (e.g., the MiProbE™) in biologically active environments. The analysis herein demonstrates decomposition of these non-selective signals into real-time metabolic activity, measurement of key biochemical processes and environmental condition parameters through classical mathematical analysis methods providing the basis of *Potentiomics* – the characterization and quantification of biochemical metabolic processes in highly dynamic non-equilibrium states.

ACKNOWLEDGEMENTS

There are innumerable people, organizations, and collaborators to thank for aiding me in my investigations of this subject as the scope of this research goes far beyond the capabilities of any single person. I would like to thank those who directly supported these investigations, aided me in developing these analysis techniques, and helped me understand the complex natural phenomena in these investigations.

First and foremost, I would like to acknowledge my three P.I.s across this scope of work, Dr. Scott Burge, the discoverer of this novel technology, mentor, and friend of over a decade, Dr. Taylor Weiss, my committee chair, research mentor, and faculty advisor, and Dr. John McGowen, who took a chance on both the sensor instrument and technology platform my team developed and have become a core research platform at the Arizona Center for Algae Technology & Innovation (AzCATI).

Thank you to my R&D hardware team of Bob Harding who designed the instrumentation electronics and Robert Blair who guided me in developing electrode designs for all the experiment deployments. Thank you to my R&D software team of David Baker, Brian Ford, and Ben Feuer who helped improve my initial analysis methods and software architecture for our open-source cloud platform which has been critical to this analysis.

Thank you to the U.S. Department of Energy (DOE) and Central Arizona Project (CAP) who directly and indirectly funded all the work herein across multiple Small Business Innovative Research awards to Burge Environmental, Inc., my employer, the DOE Bioenergy Technologies Office, and Scott Bryan of the CAP with awards to AzCATI.

A special thanks to Dr. Tom Sale and Dr. Kayvan Askarani of Colorado State University, Dr. Boyer and Al Brown of my thesis committee, Duane Barbano, Harrison Meyer, Hannah Cherry, Jimmy Jia, Philip Risser, Michell Peppers, Dave Hoffman, Dr. Russell Burge, Dr. Henri Gerken, Dr. Mark Seger, and most of all, my wife, Dafne.

TABLE OF CONTENTS

LIST OF TABLES

Table Page

LIST OF FIGURES

Figure Page

Figure Page

Figure Page

LIST OF EQUATIONS

Equation Page

INTRODUCTION

The focus of this work is to look at how to convert real-time data from dynamic systems into usable information using temporal, geospatial, or controlled variable comparison of the MiProbe signal as it relates to changes in key biological process parameters. Using classical mathematical analysis tools, the composite signal of all the complex reactions taken place can be simplified into actionable information for improving decision making or alerting to disruptive changes of interest to environmental regulations. The following sections are investigating connecting the principles of thermodynamic potentiometric measurements to the realities of needing useful real-time data for decision making, , advanced analysis based on mathematical analysis tools, applying those tools and analysis frameworks to research, and the development of new analytical tools based on those findings.

The analysis tools and frameworks herein were developed under multiple research grant awards from the DOE and CAP and provided with instrumentation systems and data-science analysis support to multiple graduate students in Dr. Taylor Weiss' lab (Weiss Lab) for their own traditional applied projects and research. The partnership between Burge Environmental, Inc., AzCATI, and the Weiss Lab has allowed for the testing of innovative ways of using the sensor technology across multiple research projects, including the early-stage proof-of-concept instrumentation systems and physical sensor probes.

POTENTIOMETRIC SENSING

Potentiometric sensors have a long and storied history as they have been a pillar of analytical chemistry since their invention over a century ago (Reedy, 1915) and eventual discovery of glass electrodes as hydrogen ion selective pH (potential of hydrogen) meters (Partridge, 1929) (Hines & de Levie, 2010). The ubiquity of such novel technology cannot be understated, from laboratories to industrial facilities to commercial and residential kitchens, potentiometric sensors are commonplace. The accuracy, consistency, and cost of such instruments coupled with the usefulness of reported parameters has made these types of meters a mainstay of industrial and environmental decision making and regulation. From Safety Data Sheets (SDS) to the Environmental Protection Agency's (EPA) Causal Analysis/Diagnosis Decision Information (Ahmad, 2006) System (CADDIS) (U.S. EPA (Environmental Protection Agency), 2022), pH is a critical component of understanding chemistry in industrial and environmental applications. Oxidation-Reduction Potential (ORP, or Potential E) is similarly used for monitoring water systems and contaminated sites as highly oxidative or reducing conditions are an indicator of the concentration of contamination. These two factors are critical to understanding chemical reactions and are commonly represented in Pourbaix diagrams (Figure 1) (Ahmad, 2006).

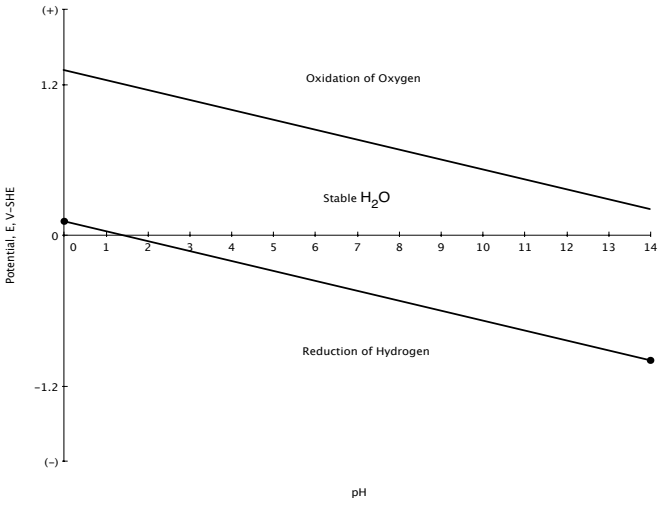

Figure 1 - Pourbaix Diagram of H_20

New developments in novel materials for both electrodes (Tom Sale, 2021) and polymer-based membranes have taken the fundamental principles of potentiometric sensors into advanced analytical fields by overcoming common problems of durability, sensitivity, and selectivity interference (A. Bratov, 2010), or inconsistent results from empirically derived equations for calculating the electromotive force (EMF) such as the Nicolsky-Eisenman equation (Eric. Bakker, 1994). These advancements are allowing the development of real-time monitoring of environmental and industrial processes or contamination sites. ORP and pH are used as discharge parameters for both municipal and industrial wastewater, and as inputs into monitored natural attenuation and environmental remediation models (Sanjay Garg, 2017). Such activities require considerable maintenance and servicing of *in situ* potentiometric sensors or are regulated to manual sample measurement which can be labor intensive and of limited value beyond regulatory monitoring applications.

Fundamentally both the reliability and selectivity of these potentiometric sensor technologies are problematic for making operational decisions in complex environmental or biological systems where control of inputs and outputs is infeasible, or maintenance and reliability issues make them impractical. Some of these issues can be resolved through engineering more complex sampling methods such as micro-fluidics equipment coupled with sample filtering and baseline reagent comparisons or automated membrane cleaning. This still requires considerable capital and maintenance outlays as well as specialized expertise in analysis for accurate interpretation. This still will not fully resolve the problems of biofouling even with the most robust potentiometric sensor electrodes in most environments. The anti-microbial platinum or silver electrode based ORP sensors which resist biofouling, are still vulnerable to their Silver/Silver Chloride (Ag/AgCl) reference electrode being biofouled or dried out from osmotic pressure differences between the reference electrode's electrolyte

solution and the environment. Further, while regular maintenance in aqueous environments can enable consistent gathering of more well understood Oxygen Reduction Potential (ORP), and pH sensors, unsaturated environments such as soils become difficult to measure overall due to losses in ionic conductivity, and overall durability issues of both types of sensor electrodes.

The use of a graphite electrodes, thought highly vulnerable to biofouling from biofilm development and of particular interest in microbial fuel cell (Diana Pocaznoi, 2012) and water treatment applications (Soumya Pandit, 2017), has revealed that after the establishment of a stable biofilm on their surface function as a non-selective membrane and present a composite signal of the aggregate metabolic activity of the biofilm as it responds to changes in the environment or microbial populations (i.e. even selectivity). After a stabilization period that can takes hours to days in aqueous environments, and up to months in dry soil environments, consistent and repeatable signals are observed that can by directly correlated with critical metabolic parameters in biologically active systems. These composite signal patterns are most prominent in photosynthetically active systems such as microalgae cultivation and plants, but also behave consistently across other microbial processes such as fermentation and anaerobic conditions.

Accelerating the establishment of stable biofilms was conducted in both aqueous and dry soil environments by using alginate hydrogels as pseudo-membrane material on graphite electrode surfaces. This was evaluated due to concerns in applying the sensing technology to high-turnover microalgae applications at AzCATI, and commercial market viability of rhizosphere sensors. Specifically, algae-pond resets and the need for contamination prevention by fully cleaning probe surfaces between strain change or harvest reset operations, and soil environments where 90-day stabilization periods would be operationally and

economically infeasible for most commercial and industrial agriculture activities. The differences in measurement variability between uncoated and coated probes was compared across multiple replicate experiments to determine the need and benefit of this pretreatment process.

Rudimentary statistical analyses were performed on these composite real-time signals to develop methodologies for comparing the change in voltage potentials rather than the absolute voltage potentials with metabolic activity of the living system being observed. This break in traditional potentiometric analysis frameworks of using the absolute value of potential measurements is due to observations that the biofilm is a living sensor membrane and not selective to any specific ion or chemical process. Higher temporal resolution investigations have revealed that signals are aggregating multiple biochemical reactions as a result of cyclical processes such as diurnal effects of day-night photosynthesis cycles and that dominant species or metabolic process in the observed environment produce distinct signal patterns at substantially different baseline potentials. Various classical mathematical analysis methods were used to amplify or filter parts of the signal to expose changes in conditions that are of operational or decision-making consequence as an attempt to create novel real-time alert and predictive analysis algorithms that would not result in false positives. The methodology here was intended to not rely on obfuscated results through overly complex custom algorithms or black-box machine-learning enhanced results that might defy belief and be largely irreproducible.

MIPROBE AND POTENTIOMETRIC SENSING

The MiProbe (Figure 2) and associated sensor instrumentation hardware (Table 1) differentiates itself from other potentiometric sensor electrodes by allowing an endemic biofilm to develop on an inert carbonaceous electrode to function as the sensing electrode membrane (Scott R Burge, 2020). Graphite electrodes have been observed to have faster bacterial cell growth rates as measured by cell density than similarly sized stainless steel electrodes in aqueous environments (Bimakr, 2018), and are commonly used with selective membranes for determination of various concentrations of chemical species (Abe, 1996) (Amini, 1999) (Ganjali, 2001). This type of biofilm formation is commonly described as biofouling of these electrodes as the open-circuit voltage (OCV) potential measurements (e.g. millivolts) against a reference electrode standard (e.g. commonly Ag/AgCL) no longer

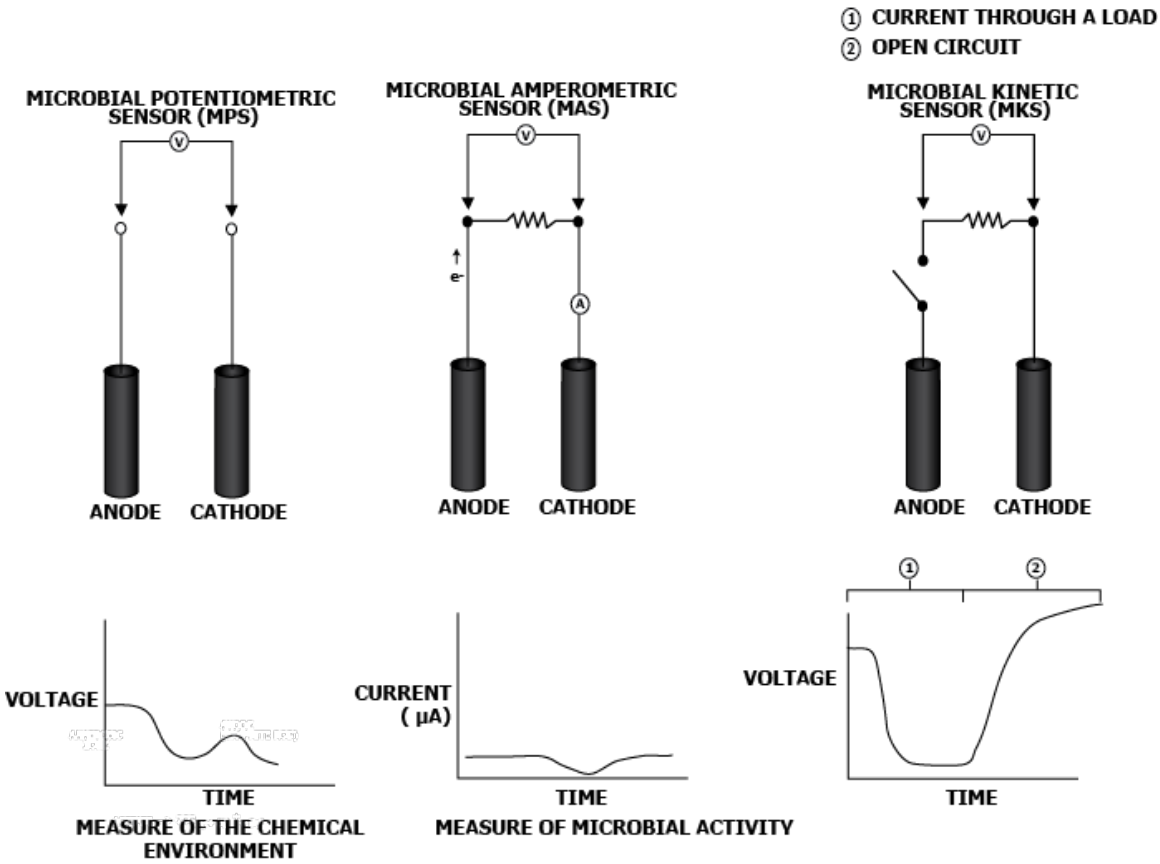

Figure 2 - MiProbe Sensor Electrodes and Measurement Types. Credit: Michell Peppers, Burge Environmental, Inc.

correspond to the absolute values associated with the oxidation reduction potentials or specific chemical potentials of the selective electrode (e.g. "sensor drift"). Both biofilm-based biofouling and adsorption of biomolecules or metabolic products create long-term maintenance issues for in situ potentiometric measurement (Lisak, 2016). Remedies to this biofilm formation or biofouling are a common area of research in environmental chemistry, electrochemistry, and analytical chemistry (Rice, 96) (Kuhlmann, 2012). Numerous techniques exist to protect potentiometric sensors from biofouling in remote monitoring applications (Delauney, 2010) and selective membrane sensor drift is of particular concern for environmental monitoring applications.

To further confound matters, OCV is an inherently ambiguous definition as while in theory it is based on the Nernst equation (Chang, 2004) which is based on a completed reaction as it related to Gibbs free energy in an equilibrium state but in practice OCV measurements are taken at intervals that are outside of controlled processes and thus are an inherently non-equilibrium state measurement (del Olmo, 2021).

Equation 1 - The Nersnt Equation

$$E = E^0 + \left(\frac{RT}{nF}\right) \ln\left(\frac{Oxi}{Red}\right)$$

"Perhaps the [Nernst Equation's] theoretically most appealing definition is that the electrochemical cell has been left undisturbed for a sufficiently long time to reach thermodynamic equilibrium." (del Olmo, 2021)

The complex interactions of biological systems and the biofilm-based membrane of the MiProbe requires analyzing the data of the MiProbe signals as a non-equilibrium state measurement and not attempting to derive specific reaction coefficients from them outside of highly controlled environments. This however does not prevent the use of analyzing the MiProbe signals in comparison to themselves geo-spatially or temporally and being able to derive actional information. In environmental, industrial bioreactor, and agricultural

applications, simplifications of this complex data into trend analysis, scale analysis, frequency analysis, and use of simple amplification and filtering techniques for rudimentary statistical analysis can provide determinative and predictive capabilities without having to precisely derive the multitudes of individual terms found in non-equilibrium reaction equations of electrical potentials or OCVs. The goal of this work is to use powerful but simple mathematical analysis techniques that can consistently and reproducibly derive key process information or parameters within the variability range of multi-day lab assays or high cost and maintenance instrumentation systems but using real-time data and rolling analysis.

Lab Instrument Boards	Inputs	Modes	Temporal Resolution	Microbial Impedence/Precision	Connectivity	Deployed	Modes
B1 (Deprecated)	*3 MiProbe/ORP/pH, 1 4-20mA, 1 Temp*	*Potentiometric*	*< 1 Second*	*1 Gigaohm, +/- 1mV*	*i2c*	*1*	*Lab*
B5 (Deprecated)	*3 MiProbe, 3Temp, 1 pH, 1 ORP, 1 4-20mA*	*Potentiometric*	*30 Minute*	*50 Megaohm, +/- 4mV*	*Serial/Cellular*	*20*	*IoT/Lab*
B9 (Deprecated)	*Expandandable*	*Potentiometric, Amperometric, Kinetic*	*1 Minute*	*50 Megaohm, +/- 4mV*	*Serial*	*3*	*Lab*
B10 (Current)	8 MiProbe, 4 ORP/pH, 4 pH/ORP, 4 4-20mA	Potentiometric	5 Minute	250 Megaohm, +/- 2mV	USB/Cellular	60+	IoT/Lab
B49 (Deprecated)	*3 MiProbe, 3 Temp*	*Potentiometric, Amperometric, Kinetic*	*1 Minute*	*1 Gigaohm, +/- 2mV*	*USB*	*1*	*Lab*
B50 (Deprecated)	*52 MiProbe, 5 Temp*	*Potentiometric*	*1 Minute*	*< 1 Gigaohm, +/- 4mV*	*Serial/USB*	*3*	*Lab*
B56 (Current)	56 MiProbe/ORP/pH, 5 Temp	Potentiometric	1 Minute	1 Gigaohm, +/- 1mV	USB	20+	Lab
B176 (Current)	176 MiProbe/ORP/pH, 5 Temp	Potentiometric	1 Minute	1 Gigaohm, +/- 1mV	USB	10	Lab
BEXP (Testing)	**23 MiProbes, 5 Temp**	**Potentiometric, Amperometric, Kinetic**	**< 1 Second**	**< 1 Gigaohm, +/- 0.1mV**	**USB/i2C**	**TBD**	**Lab**
B23T (Testing)	**16-20 MiProbes, 1 ORP, 1 pH, 3 Temp**	**Potentiometric**	**< 20ms**	**2 Gigaohm, +/- 0.03mV**	**i2c/USB**	**TBD**	IoT/Lab

Table 1 - MiProbe Instrumentation Specifications.

MATHEMATICAL ANALYSIS AND OCV

The Nernst Equation functions as a discrete measurement of voltage potential assuming at a specific point in time assuming stable equilibrium state of reactants. In this equation the electrical potential E is made up of the Environment Potential (E^0), the universal gas constant (R), the temperature (T), the moles of electrons or charge of the ion (z), and the Faraday constant or electrical charge in coulombs for every mol of reactant in the cell, and the natural log of the reaction quotient $(\ln(Q))$. In controlled benchtop experiments, Q can be two reactants added together in an aqueous solution and measured at the completion of a stable reaction against a reference electrode (E_{ref}).

Equation 2 - Complete OCV Measurment using the Nernst Equation.

$$E = E^0 - \left(\frac{RT}{zF}\right)\ln(Q) - E_{ref}$$

The terms E^0 and $\ln(Q)$ in this equation is where engineering innovation takes place to create different Type I, II, and III electrodes for determining pH, Dissolved Oxygen (DO), Chlorine concentration (Cl), etc. More advanced membrane voltage measurements use highly complex applications of the Nernst equation principles, for example, the Goldman-Hodgkin-Katz voltage equation which accounts ion-specific voltages through knowing both sides of the balanced equation in a controlled solution (John D. Enderle, 2012).

Equation 3 - The Goldman-Hodgkin-Katz Voltage Equation.

$$V_m = \left(\frac{KT}{q}\right)\ln\left(\frac{P_{Na}[Na^+]_i + P_K[K^+]_i + P_{Cl}[Cl^-]_0}{P_{Na}[Na^+]_0 + P_K[K^+]_0 + P_{Cl}[Cl^-]_i}\right)$$

With complete knowledge of inputs and a controlled experimental environment, discrete ion-specific potentials have been derived through measuring solutions at equilibrium states of stable chemical reactions. ORP and pH probes approximate these OCV measurements through repeated measurements over time intervals and reporting a stabilized measurement

value based on instrumentation firmware algorithms and the well understood potential differences of standard electrodes and hydrogen ion specific membranes.

Evaluating this change in potential (ΔE) over time using Nernst-style equations requires breaking out the actual equations to expose the underlying principle that the shared reference electrode voltage is not necessary when looking at the change in potential as it cancels out through algebraic reduction. The measurement no longer looks at the discrete millivolt values of E on a specific scale as it relates to a specific reaction potential (e.g. redox, pH values), but the change as it relates to the selectivity or ion specificity of the electrode. This temporal evaluation of ΔE is a common method to confirm measurement stability on pH and ORP electrodes.

Evaluating ΔE as a change in potential over time of an indicator electrode can be represented as:

$$\Delta E = E_{indicator\ electrode_{t_1}} - E_{indicator\ electrode_{t_0}}$$

Or, when expanded:

Equation 4 - Complete Expanded Comparison of ΔE Between Electrodes.

$$\Delta E = (E^0 - \left(\frac{RT_{t_1}}{z_{t_1}F}\right)\ln(Q_{t_1}) - E_{reference_{t_1}}) - (E^0 - \left(\frac{RT_{t_0}}{z_{t_0}F}\right)\ln(Q_{t_0}) - E_{reference_{t_0}})$$

After removing common terms such as the $E^0\ and\ E_{reference}$ electrodes:

Equation 5 - Simplified Comparison of ΔE Between Electrodes.

$$\Delta E = (\frac{R}{F}(T_{t_1} - T_{t_0})) \times (\frac{\ln(Q_{t_1})}{z_{t_1}} - \frac{\ln(Q_{t_0})}{z_{t_0}})$$

While manufacturers will not usually publicize internal algorithms of their instrumentation equipment, this temporal style of measurement of ΔE is a common way of determining measurement stability and can be a valuable tool in investigating transport phenomena at high sample rates.

As the MiProbe's OCV measurements do not map to a specific ion or reaction potential and the living biofilm membrane is inherently changing constantly, we can apply the framework that the MiProbe OCV is a direct measurement of energy state under non-equilibrium thermodynamic conditions. Using the model that the MiProbe measures energy state, we can derive useful information comparing the OCV of the MiProbe over time, geospatially, or under controlled experiment conditions (e.g. indicator electrodes in metabolically distinct but ionically conductive environments).

$$\Delta E = (\frac{R}{F}(T_{t_1} - T_{t_0})) \times (\frac{\ln\left(Q_{t_1}\right)}{z_{t_1}} - \frac{\ln\left(Q_{t_0}\right)}{z_{t_0}})$$

This will not work with any Nernst-like equations, despite the measurement instrumentation being identical. While R and F, are known constants, and T can be directly measured, the reactant quotient Q and electron concentration z side of the equation cannot be further derived as neither variable can be measured nor is the reaction at a stable equilibrium state at either t_0 or t_1. It's also possible that a Type IV non-selective biofilm membrane electrode would have more a more complex equation than can presented here. ΔE can however still be used to evaluate key biological process parameters using known temporal intervals of changes in biomass, nutrient concentration (e.g. reactants), and metabolic pathway (e.g. photosynthesis or respiration), and the resultant changes in potential energy of the cell. This composite of change in potentials, P, can be represented as an incomplete and simplified equation:

Equation 6 - MiProbe ΔE Conceptually Equation.

$$\Delta E = \Delta(P_{biomass} + P_{reactant} + P_{Metabolism} + \ldots)$$

The net change, or ΔE represents the change in both biomass concentration and metabolic activity (e.g. chemical reactions) in a composite signal of a non-selective membrane electrode. In this case, ΔE is made up of Potentials (P) of environmental conditions (e.g.

chemical reactants outside of biological activity), biomass, and the net reaction of the biomass' metabolic activities. These aforementioned potentials are not indeterminant but not necessarily differentiable and provide a composite signal. By using the ΔE of electrical potential measurements over process specific time intervals it is possible to transform these real-time measurements into datasets for other types of classical analysis that correlate strongly with key performance and operating parameters of biological systems. The other terms (e.g. "…") that may affect ΔE are indeterminant at this time as they may be within the margin of error when comparing this composited signal to standard lab assays (e.g. Ash Free Dry Weights, Cell Counts, etc.) or other selective measurements.

This work will investigate three principal ways of evaluating ΔE and how it relates to biological metabolic activities across time, space, and variable controls as the basis for the concept of Potentiomics. These methods represent building blocks for more complex analysis and can be used in conjunction with each other. The fundamental equations which can be simplified and adjusted to these various measurements across time, space, and controlled environments. These equation function as rudimentary definitions of comparisons of ΔE that are used in more advanced analysis techniques in this work. These equations are intentionally shown using basic algebraic forms to provide an approachable framework for practitioners, graduate students and researchers without having to resort to more complex calculus-based approaches.

Essential Methods of Evaluating the Change in MiProbe Signals

Equation 7 - Expanded Change in Energy (ΔE) with Respect to a Reference Electrode.

$$\Delta E = (E_{electrode_i} - E_{reference_i}) - (E_{electrode_i} - E_{reference_i})$$

and simplified into the three principal analysis components:

Equation 8 - Change in Energy (ΔE_t) with respect to Time

$$\Delta E_t = E_{electrode_{t_1}^x} - E_{electrode_{t_0}^x}$$

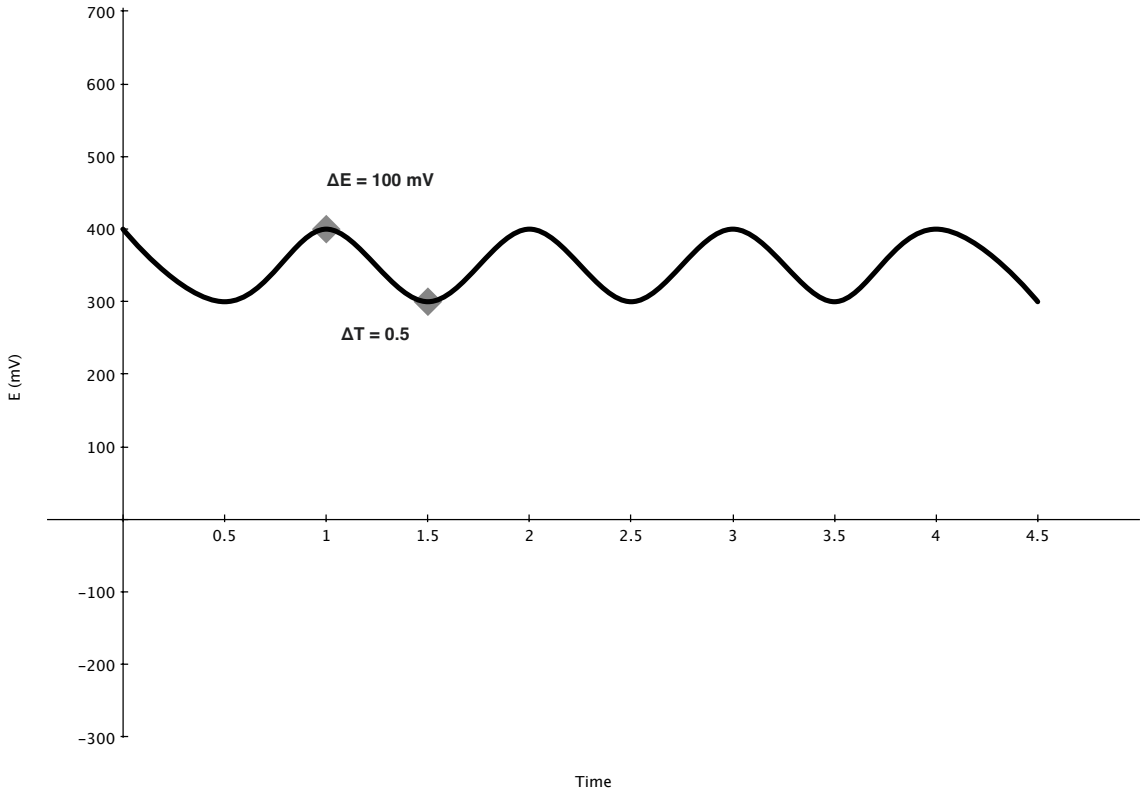

Equation 9 - Change in Energy (ΔE_x) with Respect to Geospatial position.

$$\Delta E_x = E_{electrode_{t_0}^x} - E_{electrode_{t_0}^y}$$

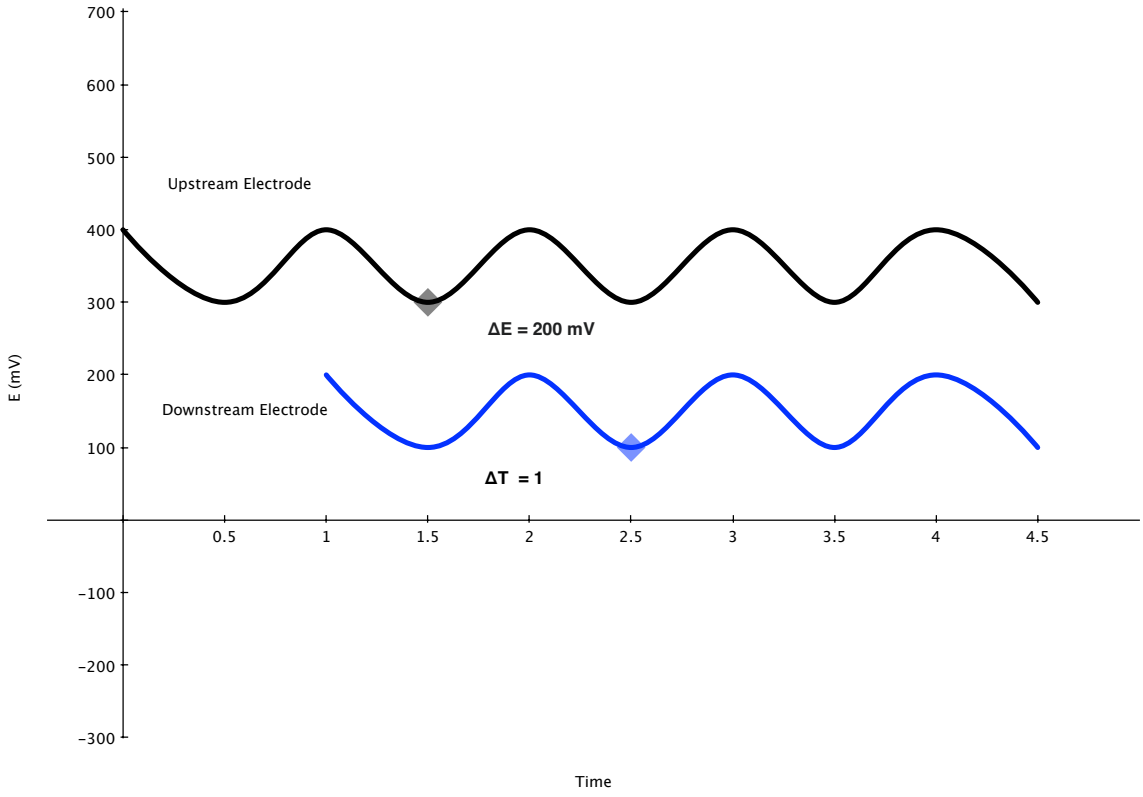

Equation 10 - Change in Energy (ΔE_m) with Respect to Metabolic Differences.

$$\Delta E_m = E_{variable\ electrode} - E_{control\ electrode}$$

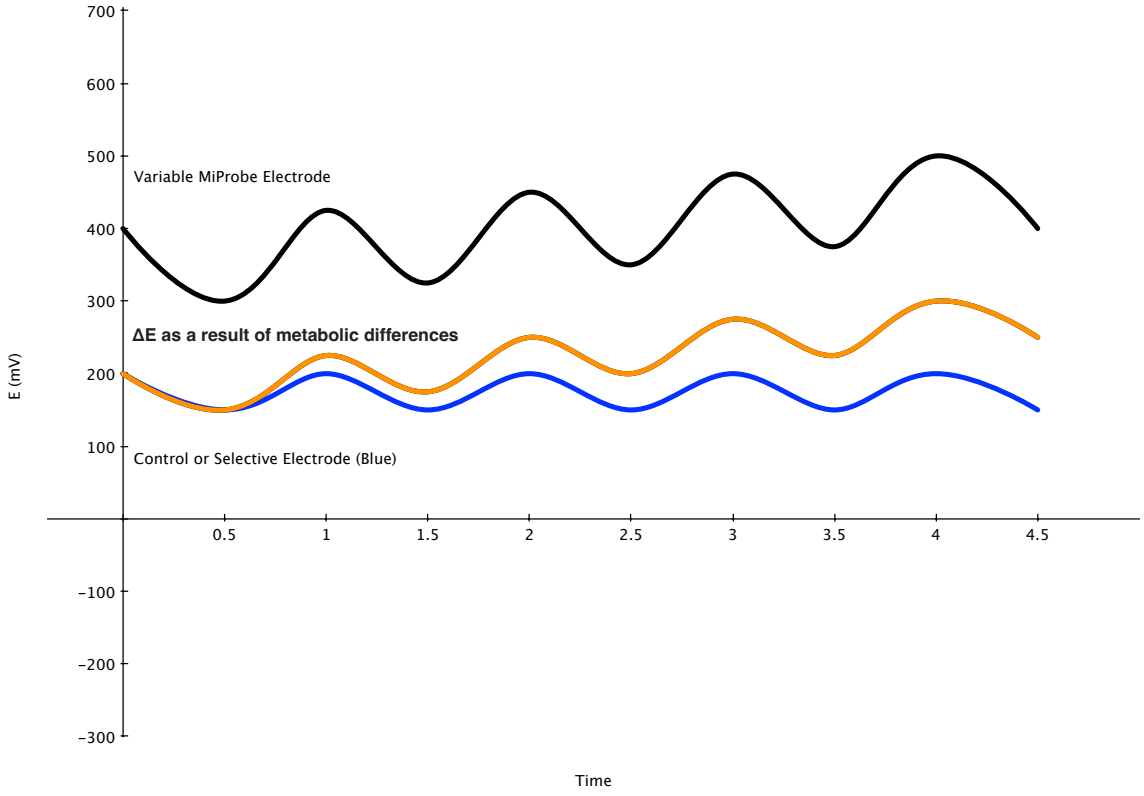

Combinations of these principal equations can be used to trace algae blooms through large water systems, nutrient loading through a wastewater system, predict change in biomass over time in bioreactors, or filter or amplify differences in metabolic activity within an experimental environment.

Time Series Analysis

Large datasets of real-time measurement data are providing scientists, industrial operators, and regulators new tools in understanding changes in environmental conditions and critical biological or ecological processes. The quantity of measurement using high-frequency real-time measurement aids in reducing measurement error and noise within data as compared to conventional sample analysis datasets (i.e. smoother data) (Philippe Esling, 2012). In ecological systems where traditional lab replicate analysis cannot be performed such as riverine and canal systems or municipal wastewater treatment plants, time series analysis of repeating and changing patterns of behavior is key to understanding underlying conditions. Looking at changes over time of common sensor instruments reveals metabolic activity through either indirect measurement of environmental variables (e.g. ORP, pH, DO, Temperature) or the direct measurement of biological indicators (cell counts, biomass dry weights). Real-time data streams coupled with time series based statistical analyses can allow for early warning detection of major disruptions to biological environments (Vasilis Dakos, 2012)or industrial processes. Most importantly, the change in OCV values of MiProbe signals (ΔE) is complementary to time series-based analysis over discrete analysis of single measurements (e.g. pH) for making decisions in regulatory or process control systems.

Classical Statistical Analysis

To remove error, noise, and enhance understanding of the underlying MiProbe OCV signals, rolling statistical analyses on these time-series data sets are performed. At a fundamental level OCV instruments all use rolling statistics in to acquire stable measurements or de-noising electronics-based signals (e.g. temperature induced or AC-current derived noise sources) (Huixian Ye, 2019). Rolling standard deviations, variance, averages, minimas, maximas, and other classical statistical analyses can be performed to detect changes in environmental conditions (Figure 3) (Vasilis Dakos, 2012) or to directly monitor metabolic activity of the MiProbe or indirectly extract functional information. Deciding on the period of analysis is important for creating actionable information from these statistical analysis tools.

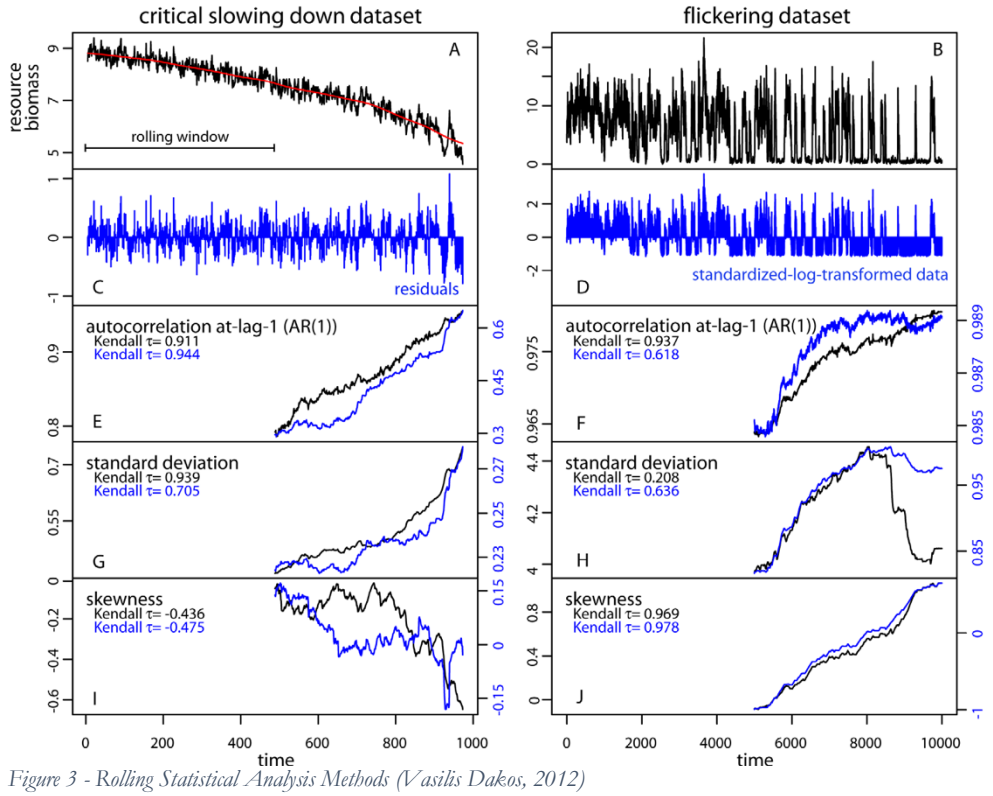

Figure 3 - Rolling Statistical Analysis Methods (Vasilis Dakos, 2012)

Classical Decomposition

The composite signal of multiple metabolic and environmental factors of the MiProbe signals can be used as a way of filtering and amplifying portions of the MiProbe signal that correspond to parameters of interest. The basis of this statistical decomposition technique has been used for nearly a century (Anderson, 1927), and is now a fundamental analysis used in forecasting and predictive models (Rob J. Hyndman, 2018).

The additive model (Equation 11) for classical statistical decomposition is composed of the raw data y_t which is made up of a seasonal component S_t which is a repeating pattern based on a supplied pattern (e.g. diurnal, annual, hourly, etc.), the trend T_t which is a rolling average, and the residuals or error E_t, which is the remainder of the signal not accounting for in either seasonal or tend components.

Equation 11 - Classical Decomposition Additive Model Equation.

$$y_t = S_t + T_t + E_t$$

Building real-time rolling statistical analysis models for detecting disruptive events to wastewater treatment systems can help identify the dumping of chemical contaminants that can harm both operations of the biological processing and nutrient removal and the effluent parameters of the treated waste out of discharge regulations. Applying a statistical filter to decomposed signals can be used to create automated alert thresholds of real-time data platforms to aide stakeholders in making sampling or process decisions. The residuals remaining after subtracting the trend T_t and the normal diurnal pattern S_t are of special interest in automating alerts for wastewater applications (Figure 4, 5, 6). As the residuals are a change from 0 after removing the T_t and S_t, simple automated alert thresholds can be used based on a rolling standard deviation filter (Figure 5).

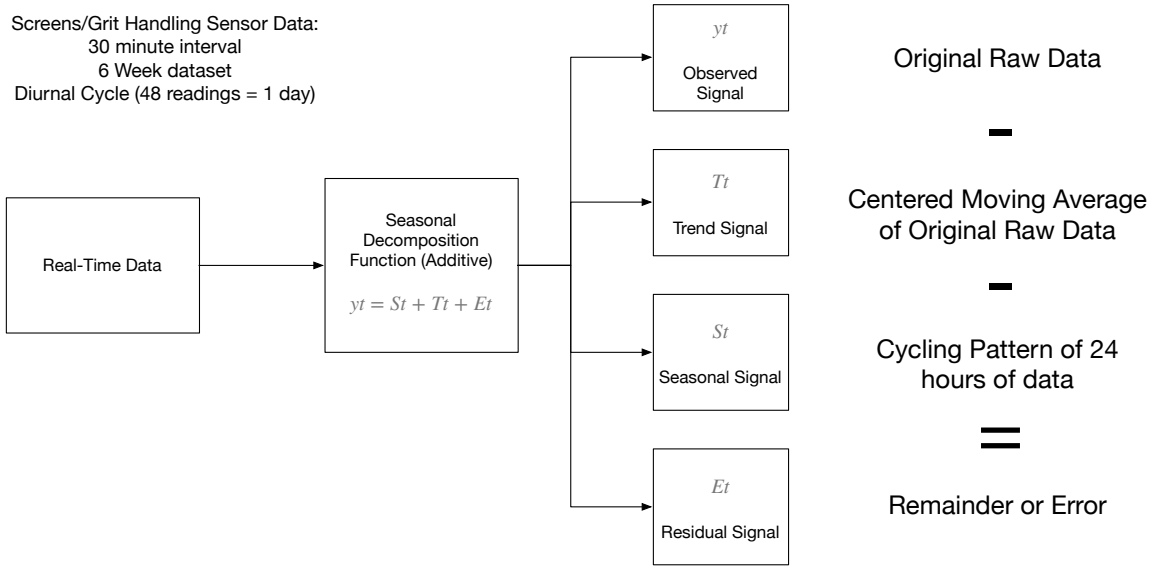

Figure 4 - Seasonal Decomposition as Applied to the Headworks of a Wastewater Treatment Plant in Arizona.

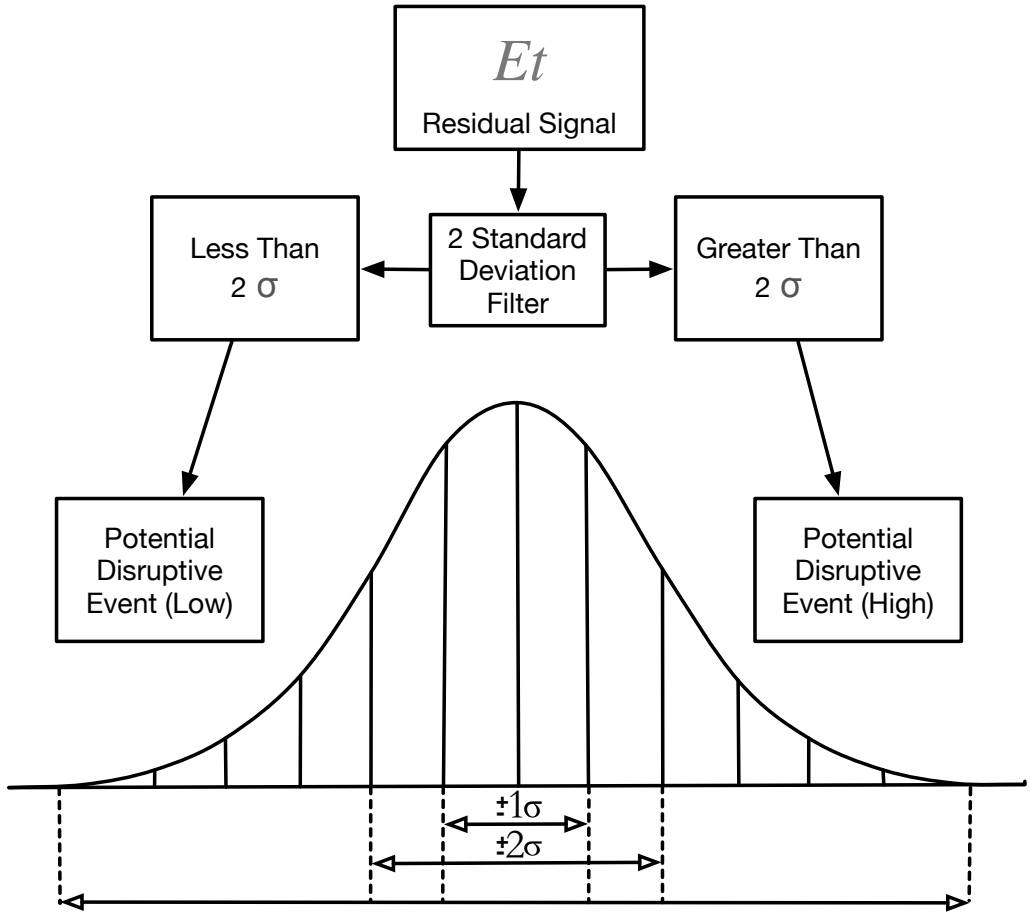

Figure 5 - Automated detection of disruptive events using the residual signals and a rolling standard deviation filter.

=

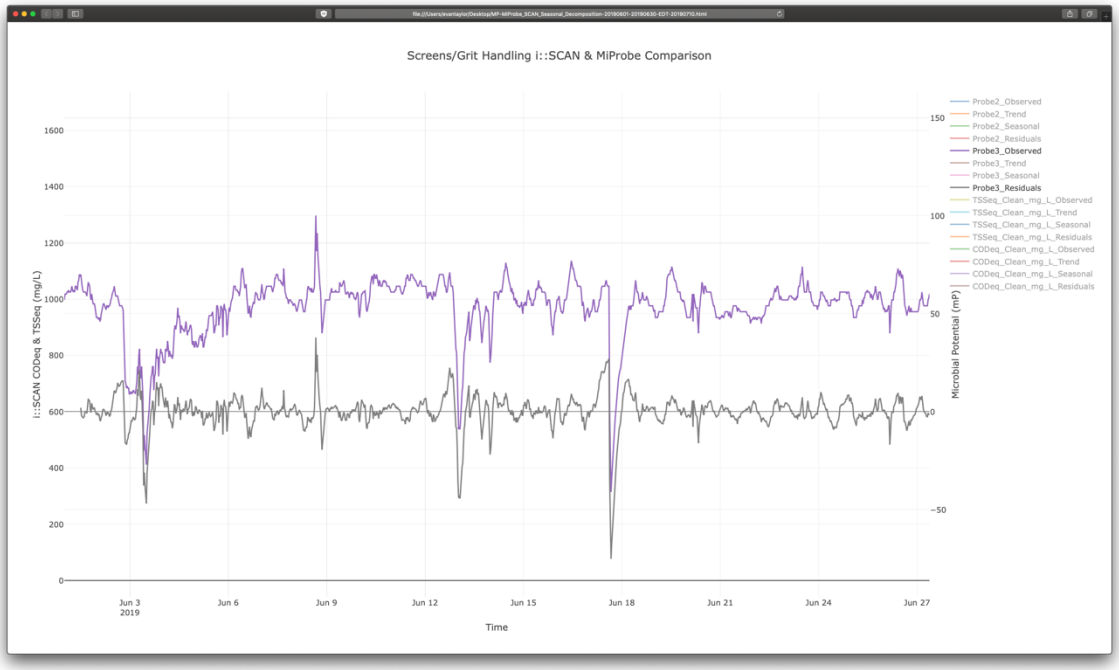

Figure 6 - Comparison of Observed and Decomposed Residuals of MiProbe Sensor Data from a Wastewater Treatment Plant.

Fast Fourier Analysis

Determining seasonal periods for classical decomposition, or time intervals for investigating metabolic activity of MiProbe signals requires a quantifiable and repeatable methodology. The Fast Fourier Transform (FFT) is a common numerical analysis tool (Ziegler, 1972) for identifying the periodicity of signal patterns within timeseries data (Like Gao, 2002), and is commonly used in biological signal analysis (Harris, 1998). Running an FFT on real-time data of 3 weeks of algae growth in a well-mixed controlled chamber with a distinct diurnal pattern (Figure 7) reveals multiple periods with amplitude signals that can be associated with controlled variables such as 12-hour light cycles. This diurnal pattern is revealed in the FFT at the .5 day or 12-hour mark (Figure 8), accounting for the diurnal variability of the signal, while an approximately 30 +/- 5 minute signal is observed which relates to the constant variability within the signal pattern (Figure 9). Without assuming these amplitude spikes are directly related to any specific metabolic function, an FFT can be used as a basis of choosing

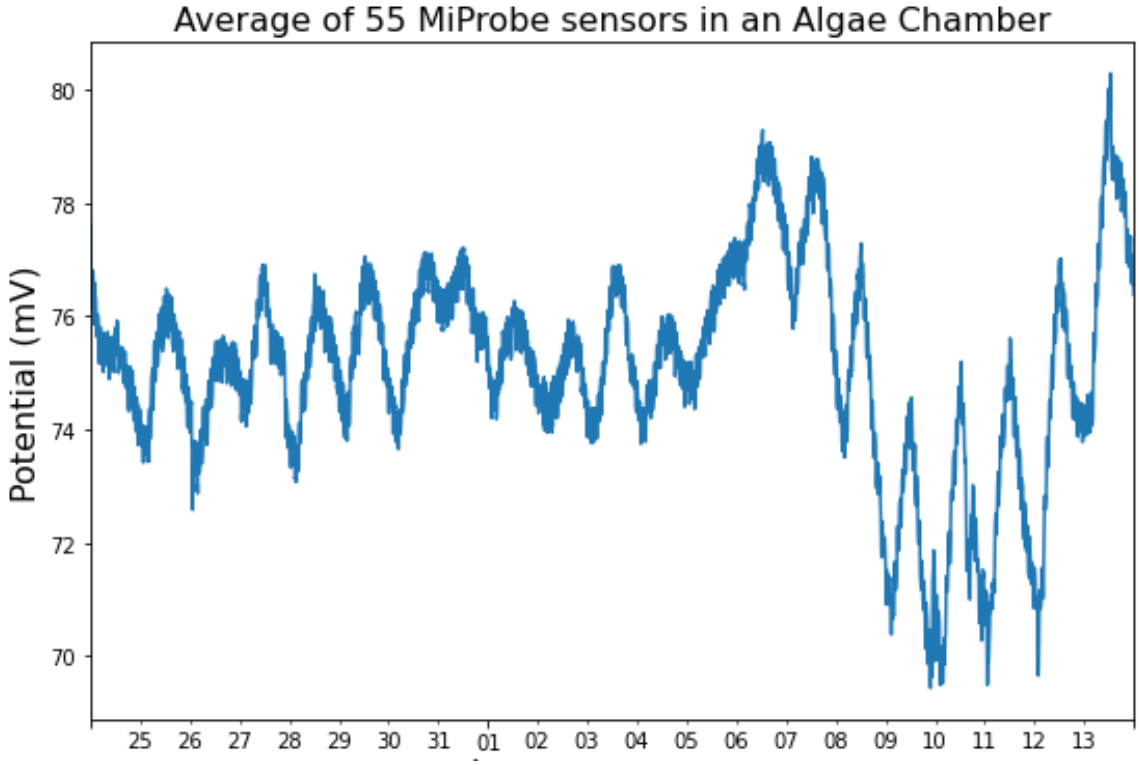

Figure 7 - Timeseries Data of the Average a 55 MiProbe Array's Signals in an Algae Chamber.

temporal intervals for seasonal decomposition, intervals between various statistical analyses, and identifying periods for investigating further metabolic activity. The figures herein are provided as example analysis from ongoing research to demonstrate the statistical methodology that will be applied to other datasets.

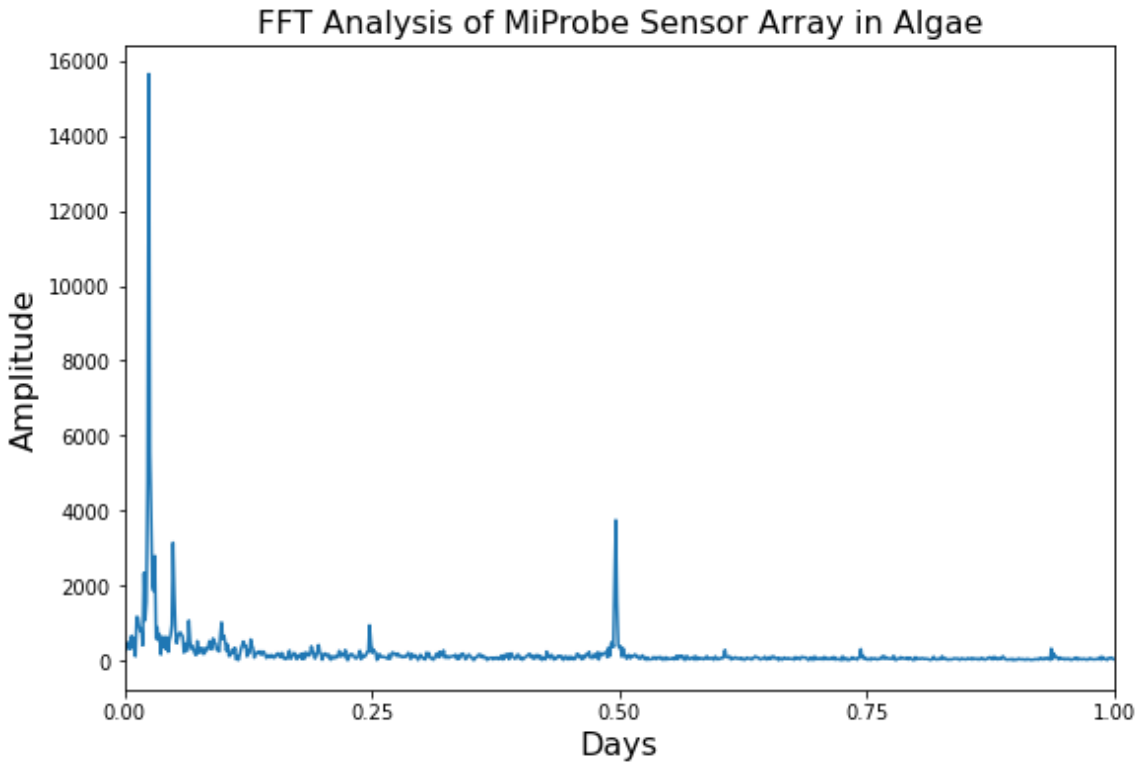

Figure 8 - Fast Fourier Transform of Average MiProbe Array Data (24-hour Window).

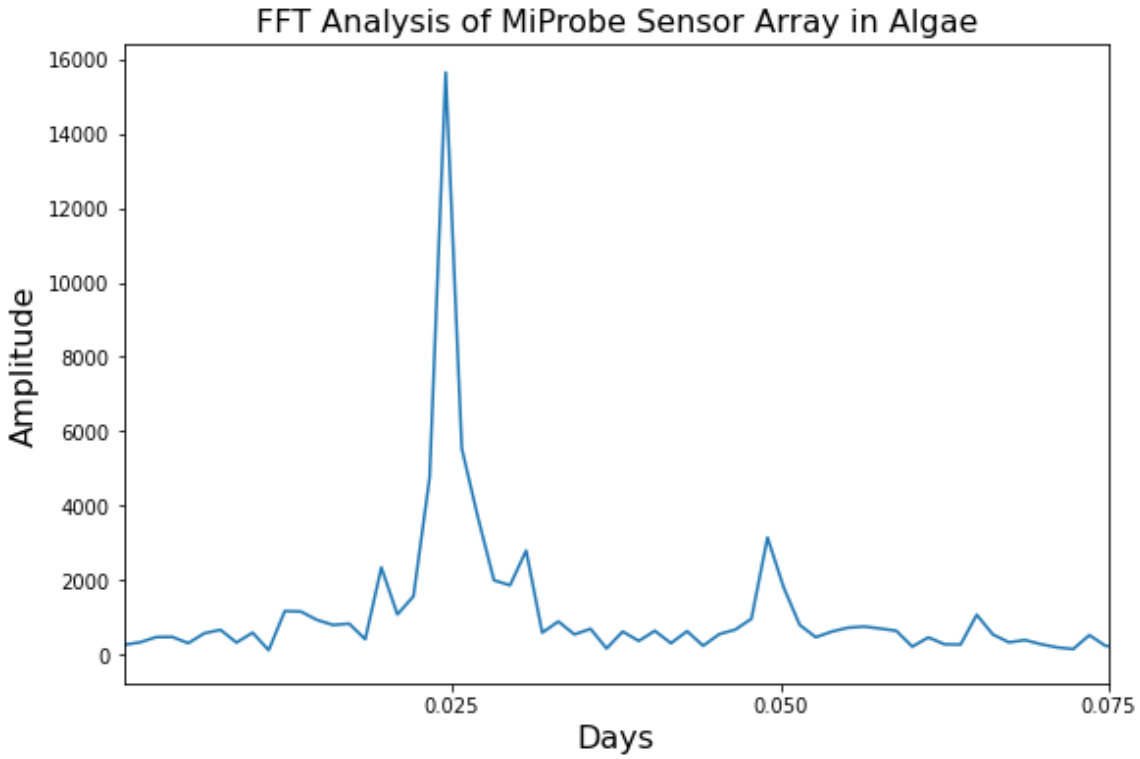

Figure 9 - Fast Fourier Transform of Average MiProbe Array Data (<2-hour Window)

Predictive Models

Taking these timeseries analysis methods for identifying temporal patterns, statistical relevance to both operational and regulatory concerns, basic predictive modeling tools provide the next step in providing useful data for decision making. Rolling analyses can be used to create real-time predictive forecasts that can be the basis of more advanced alerting, confirm tracing of biomass and nutrient loads through industrial processes or water systems, and as the basis of assisted learning models of Machine Learning (ML) and Artificial Intelligence (AI) tools.

The Holt-Winters predictive algorithm (Anne Koehler, 2001) is commonly used in climate-forecasting models (Liljana Ferbar Trater, 2016) and has established itself as a standard model to utilize in seasonal forecasting across multitudes of disciplines (Howard Grubb, 2001). The simplicity of the model is of specific interest as the multiple factors influence the MiProbe signal cannot be known. This provided a simple starting point for analyzing the predictive capabilities of the MiProbe metabolic signals.

IN SITU OBSERVATIONS AND IN VITRO EXPERIMENTS

Central Arizona Algae Bloom Monitoring

The following evaluation of predictive modeling of Central Arizona Project (CAP) canal algae bloom monitoring data was conducted using a combination of seasonal decomposition and Holt-Winters' Exponential Smoothing algorithm's additive method (Meyer, 2021). The trend, diurnal pattern and residuals were extracted from the raw signal for the MiProbe near the surface of the canal system near Lake Pleasant in Arizona (Figure 10). During the evaluation of decomposing the raw Lake Pleasant data, changes in flow coinciding with operation changes in April (flow increases from the reservoir), and a later event of an unforeseen water release was observed to impact signals in the MiProbe trend and residuals.

This was effectively applying a rolling average to subtract the trend of baseline MiProbe signals, and amplify the portions of the signals directly related to algae photosynthetic activity and nutrient (or operational) changes. A forward prediction of using 3 weeks of prior decomposed diurnal and residual signals are used as training data to forecast 7 days of the canal bloom (Figure 11). A disruption from intrusion of water into the canal system on May 17th was noted upstream of the sensor system that required maintenance on the canal system disrupting normal flow later in the month.

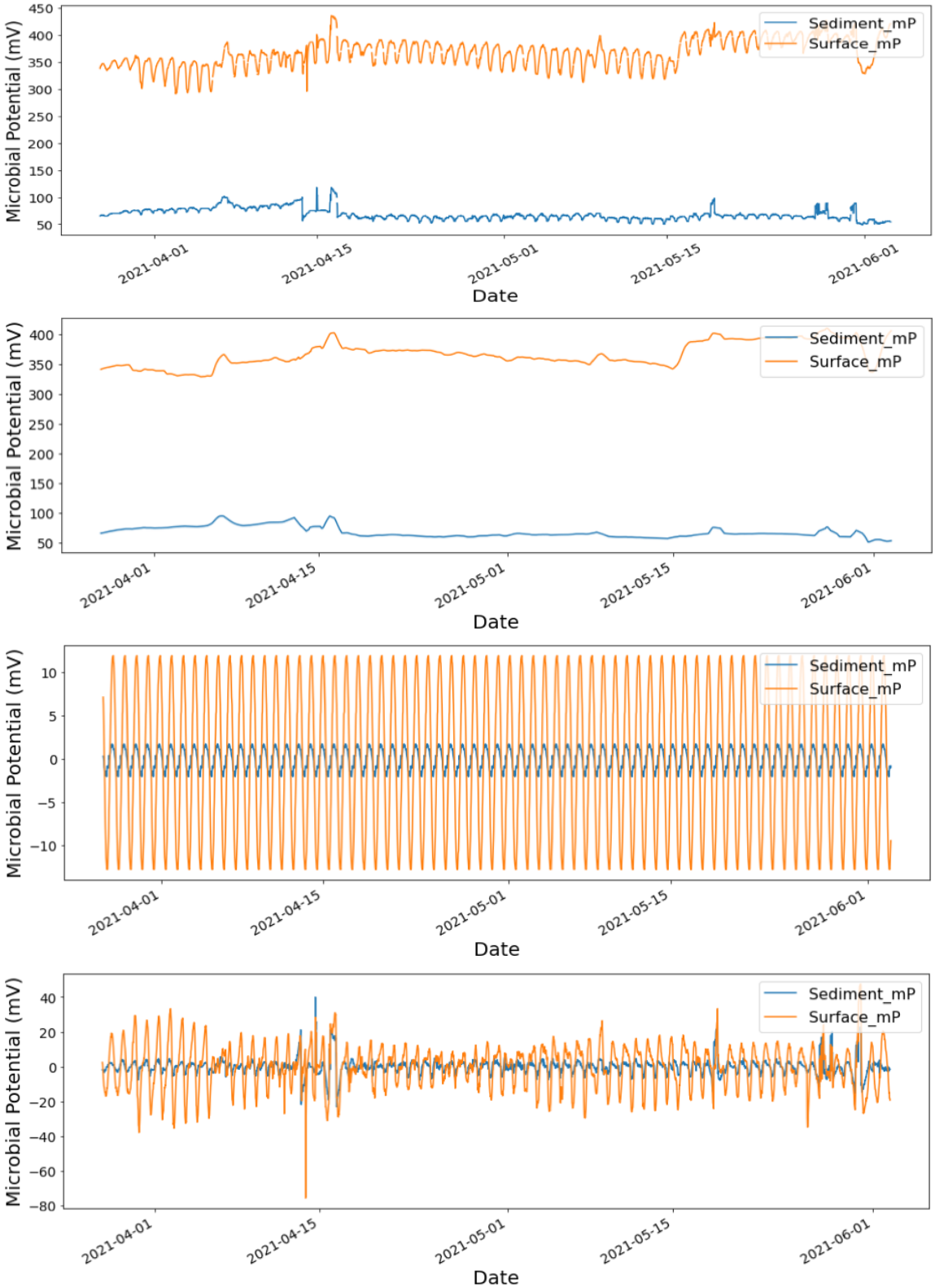

Figure 10 - Decomposition of Real-Time MiProbe Sensor Data on the CAP Canal (Meyer, 2021). Top-Bottom: Raw Observations, Trend, Normal Diurnal Pattern, Residuals.

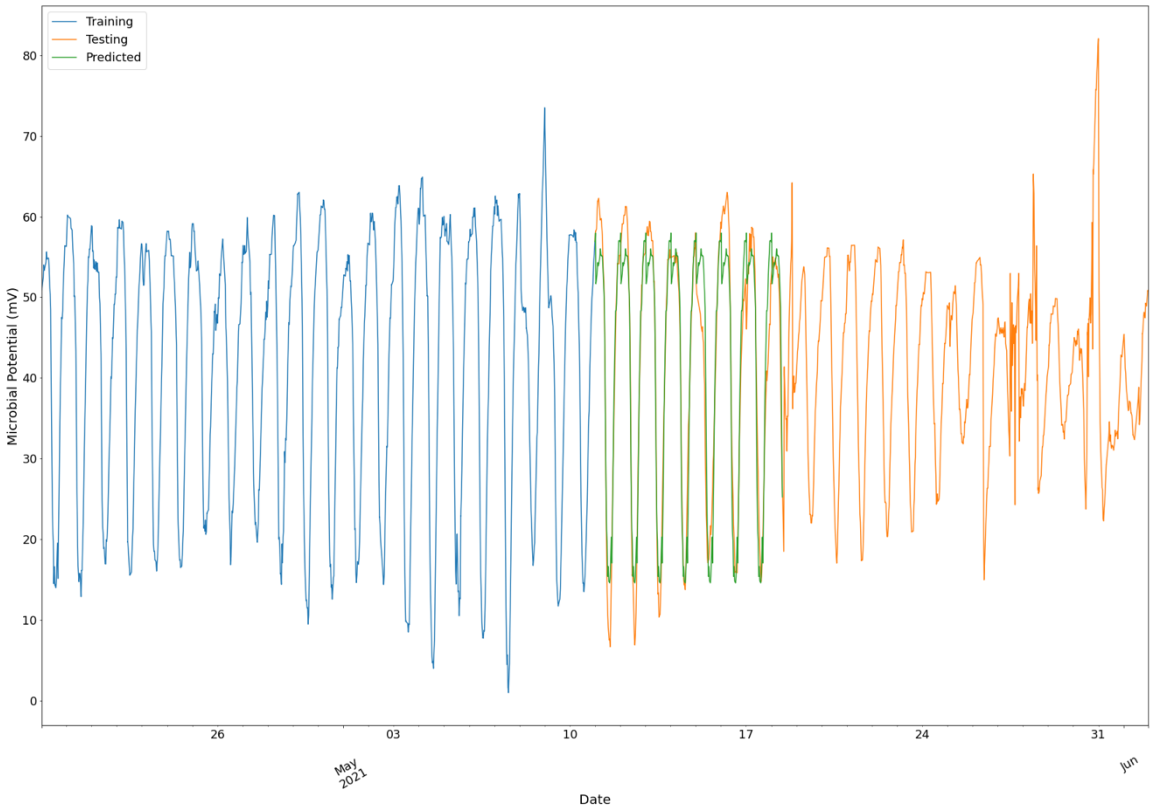

Figure 11 - Holt-Winters Model as Applied to Recomposed Seasonal + Residuals Data (Meyer, 2021).

Expanding on this work, further evaluation of creating an automated alert trigger using these predictive methods was applied. Ten days of prediction using the previous methodology were applied to see how accurate the prediction in algae metabolic activity would perform and if it could be used as an automated indicator in real-time monitoring applications (Figure 14). A rolling correlation between the Prediction and Testing (e.g. real-time data) series using the last 24 hours of datapoints of both produced significant drops in prediction correlation (Figure 13) prior to the detection of the water intrusion event on May 17th and a severe drop in correlation between predicted pattern behavior and real-time data. The preceding drop on the 15th and 16th coincided with a severe storm event which was the root cause of the down-stream water intrusion event (Figure 12). The larger drop in prediction correlation takes place during an interruption in flow to allow maintenance work in response to the intrusion event. This early drop in correlation of MiProbe sensor prediction data can be used to alert to severe changes in environmental or operational conditions enabling faster response to operational disruptions and prevent or lessen intrusions into the canal system.

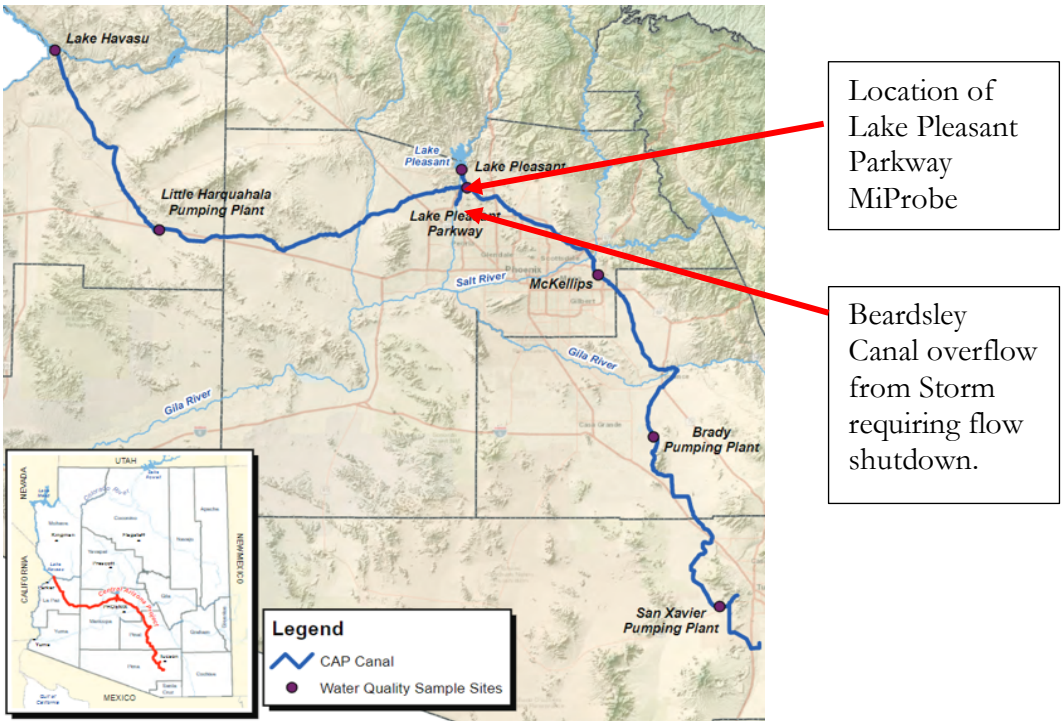

Figure 12 - Central Arizona Project Canal Map (Credit: CAP)

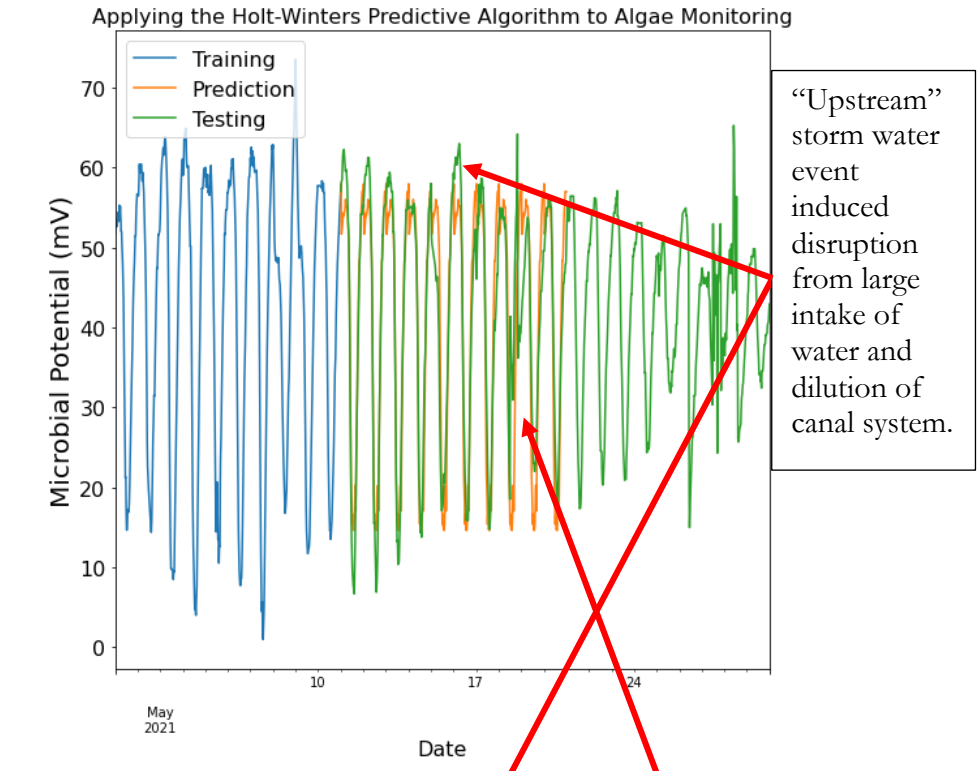

Figure 14 - Expanding the Holt-Winters prediction.

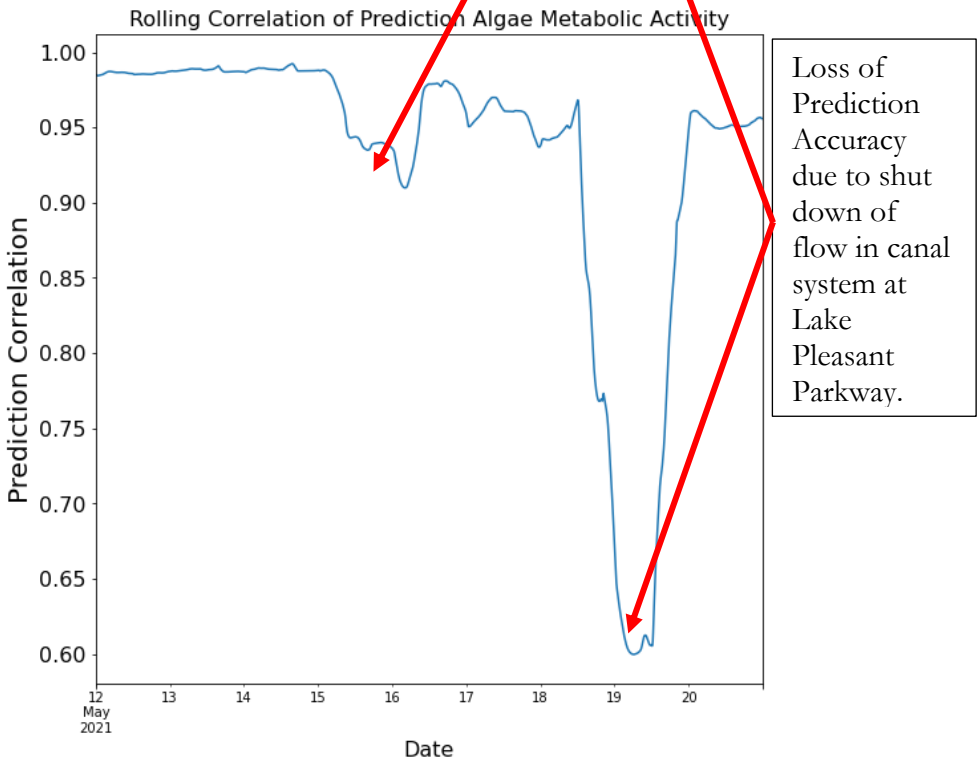

Figure 13 - Rolling window corellation between prediction and test (real) data.

Rhizosphere Applications

Background:

Biofilm formation and stabilization in aqueous environments has been observed to take place within 24-48 hours in algae raceway ponds, however dry soil environment present difficulties in achieving stable MiProbe signals on commercially feasible timescales. Additionally, while insertion of probes into the rhizosphere had been demonstrated in during a DOE SBIR investigations of Phase I, II, and IIB research awards for monitoring the saturated and unsaturated zones for environmental, applications in soils the minimum times before stable signal could be observed were in 1-3 months. This may be an acceptable stabilization for long-term environmental and ecological system monitoring using low-zero maintenance probes but would be non-viable for agricultural applications.

An early milestone of a DOE BETO investigation was to assess if the MiProbe sensors could stabilize quickly enough for 3-5 day harvest resets, and 1-week cultivation studies. Previously stabilization periods in riverine and potable water monitoring systems had been observed to take up to a month while wastewater systems, depending on process, would take between 1 and 14 days before stabilization of the MiProbe signal could be observed. Coating probes with an alginate hydrogel was investigated in both these applications to provide a scaffold structure for accelerating microbial growth as well as a nutrient source. To test if stable signals could be measured quickly a proof-of-concept experiment using a seedling tray and coated and uncoated graphite electrode.

Proof-of-Concept Methods:

An alginate coated graphite electrode and an uncoated graphite electrode were inserted into a Root Riot™ peat seedling pod and hydroponics seedling tray with an ORP and previously stabilized (2-weeks in the seedling tray) uncoated graphite electrode in the water to investigate stabilization period signal changes as a proof-of-concept. The seedling tray maintained a 2cm water depth and the Ag/AgCl reference electrode of the ORP was used as a shared reference between all graphite and ORP indicator electrodes. The system was setup inside an enclosed Percival incubator chamber set to 31C and 90% humidity with 1.5% atmospheric CO_2 being maintained and lighting on a 12-hour day-night cycle using a TP-Link™ Kasa HS105 programmable wifi-outlet controlled a Giixer 1000W LED light suspended 45cm above the seedling tray.

Data Acquisition:

Real-time humidity and temperature were measured using a DHT22 sensor, and two PiCamera NoIR was setup to store imagery data. MiProbe and ORP data were acquired using a Raspberry Pi 4 and a MiProbe B56 sensor instrumentation board. Both imagery and sensor data were recorded every 5 minutes to an AWS cloud platform using DynamoDB and S3 storage buckets for sensor data and imager respectively.

Measurement Confirmation:

A high impedance Milwaukee™ MW500 ORP meter and a Fluke™ 79 Series II Multimeter were used to confirm conductivity between reference electrode and indicator electrodes (both ORP and Graphite) through the seedling trays and into the seedling pods. Upon the 2nd iteration, a tomato seed was bonded to the alginate hydrogel.

The alginate coating and seeds were prepared identically to Deyang Qi's later Thesis work methodology (Qi, 2021) below:

Preparation of Alginate:

3.3 g of sodium alginate (Alginic acid sodium salt from brown algae, BioReagent, suitable for immobilization of microorganisms, Sigma-Aldrich) and 4.3g of MOPS were dissolved in 225 ml water. Then the suspension was stirred at 180 rpm and 95 °C until completely dissolved. The dissolved gases during the stirring process in the alginate solution were removed with a vacuum pump. Then, the alginate solution was sterilized at 121 °C for 30 min. A $CaCl_2$ solution was prepared by dissolving 2.49 g $CaCl_2$ and 4.7 g of MOPS in 225 ml DI water. The solution was autoclaved at 121 °C for 45 min.

Seed Coating Preparation:

The seeds of tomato 'Golden Jubilee' (Marde Ross & Company) were surface sterilized with 30% bleach for 15 min, then washed 3 times with sterile water. Coating of seeds were carried out under sterile conditions in a laminar flow hood. The alginate was added dropwise with the aid of a 10-ml sterile syringe on the tomato seeds and the probe surface. The coated seeds and probes were then bonded together, by soaking in 0.1 M $CaCl_2$ solution to form the alginate hydrogel. The excess Ca2+ ions were washed out with sterile tap water after 3 min of the formation of alginate hydrogel.

Initial Results:

Immediate signal similar to the previously stabilized graphite electrode in the water tray, while the uncoated electrode took 4 hours to achieve its baseline magnitude but did not show the same variability as the other graphite electrodes (Figure 15). Signal behavior was largely unchanged for the following 2 weeks of monitoring after this 4-hour window. Repeated confirmation of OCV measurements and conductivity were completed using high impedance meters.

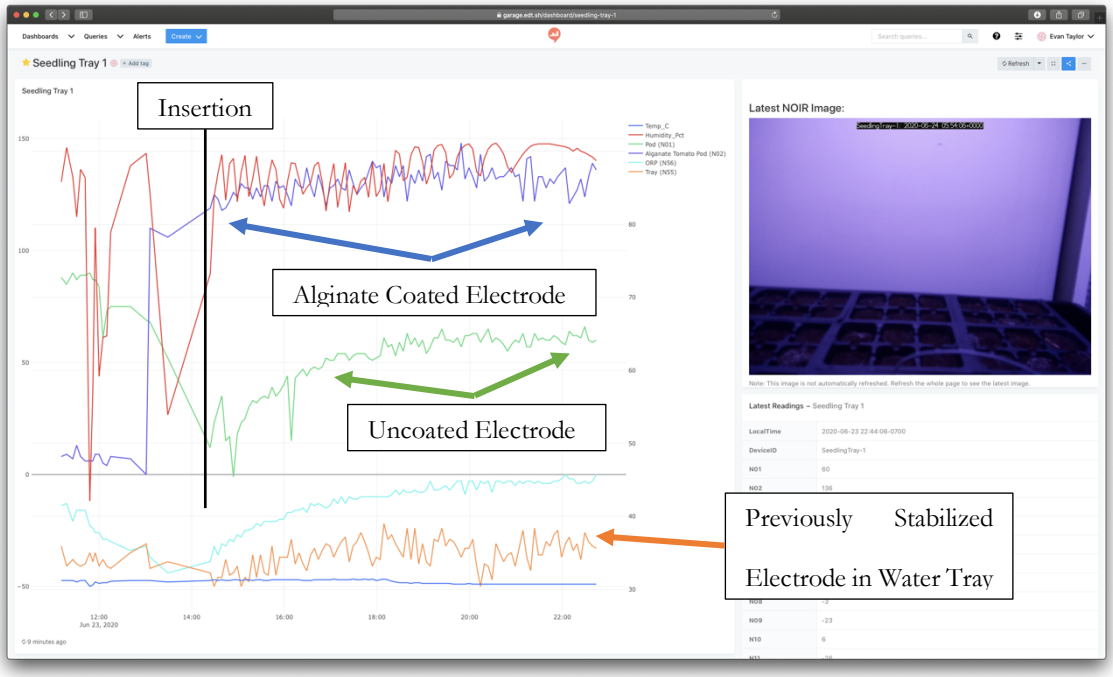

Figure 15 - Initial Testing of Alginate Coated Electrodes in a Hydroponic Seedling Tray.

Proof-of-Concept with Seed Results:

After successful signal differenced and conductivity with the experimental apparatus was confirmed a repeat of this initial experiment with this time the seed directly bonded to the graphite electrode (Figure 16, top). Initial results were identical, however upon germination of the seedling variability and baseline signals shifted. Upon closer inspection, a 12-hour cycle pattern matching the light timing of the incubator appeared (Figure 16, Bottom). Both variability and baseline signal patterns appeared to change during these 12-hour cycles of the seed-attached electrode.

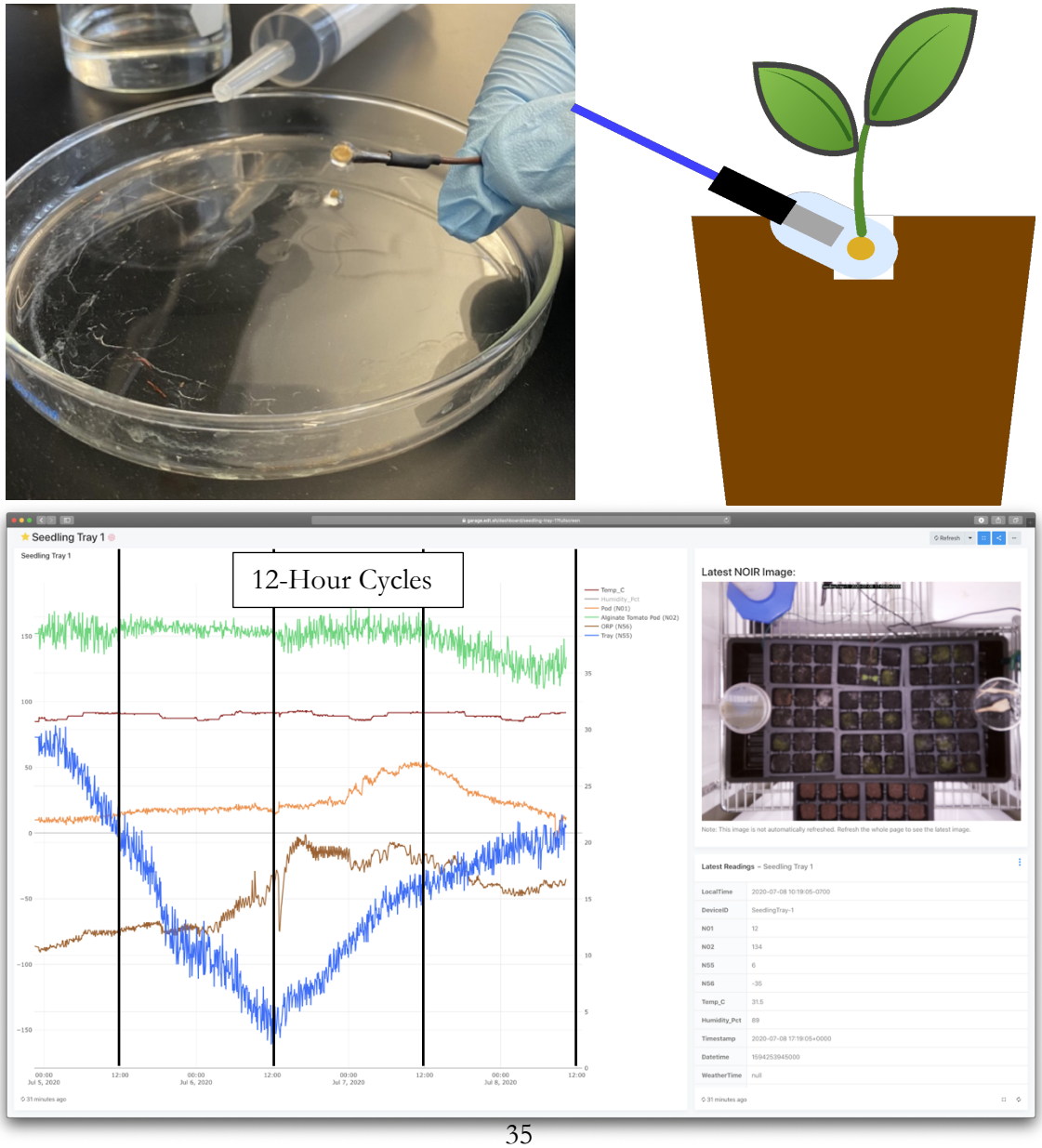

Figure 16 - Clockwise from top: Bonded Tomato Seed to MiProbe, Figure of Bonded Seed and Peat Pod, Real-Time Dashboard of First Seeded MiProbe and Comparison Electrodes.

An Expanded Proof-of-Concept:

After initial confirmation of the principles that the MiProbe with an alginate hydrogel coating could discern signal patterns within the first 2 weeks of germination of a directly attached seed (Figure 17), an expanded investigation was planned to confirm differences between coated and uncoated probes in seeded and unseeded pods under identical conditions. Upon initial inspection there were no discernable signal pattern differences in the raw measurement data. While an underlying diurnal pattern could be discerned in the raw signals, metabolic differences from treatment types were not clearly differentiable (Figure 18).

Figure 17 - Seeded and Unseeded Coated and Uncoated Probes in Randomized Tray Experiment (Qi, 2021)

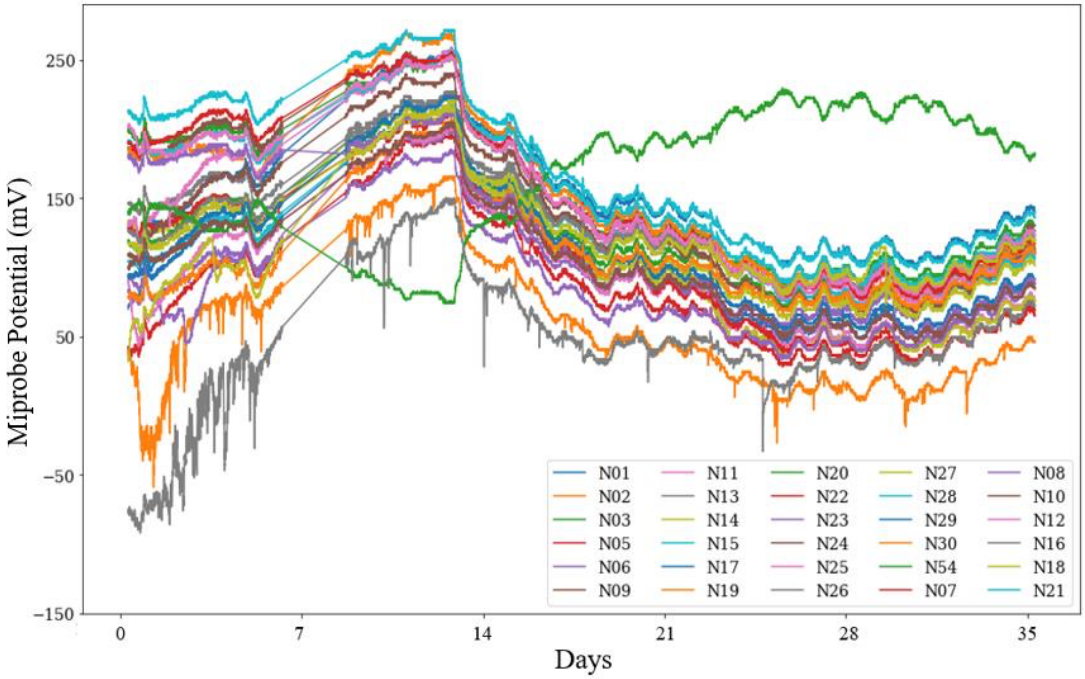

Figure 19 - Real-time Seedling Pod Data of Coated and Uncoated Probes (Qi, 2021).

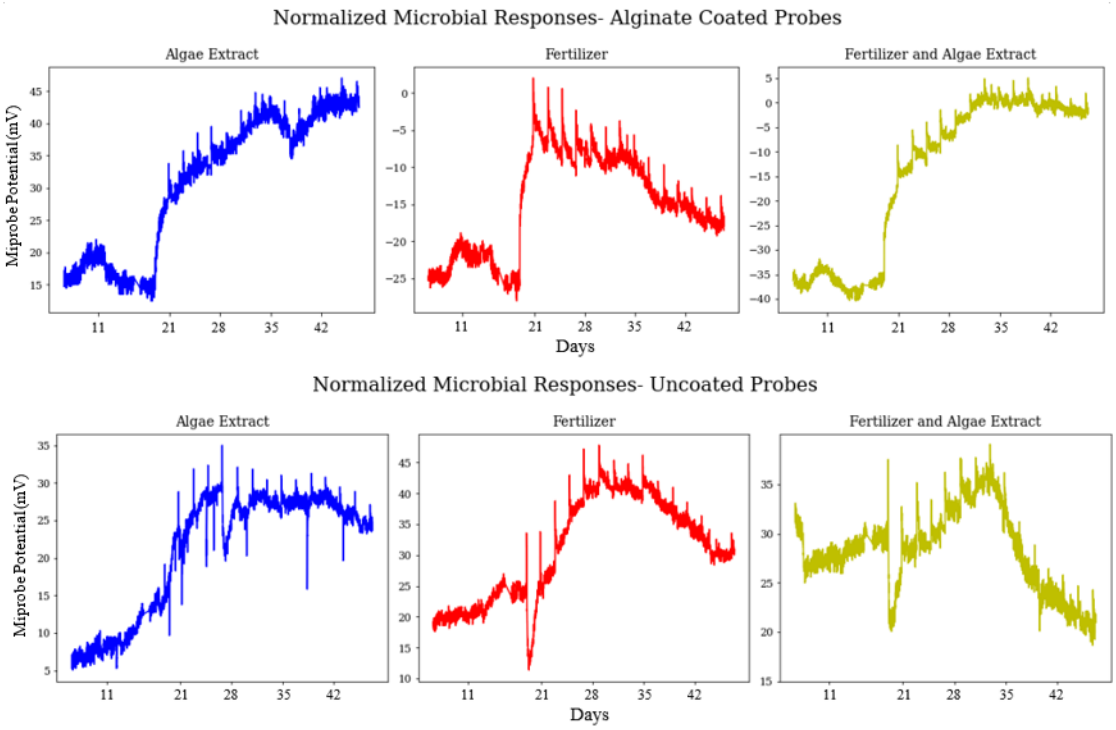

Figure 18 - Average of Normalized Coated and Uncoated MiProbes Categorized by Treatment (Qi, 2021).

Using the combined averages of the germinated seedlings by treatment (e.g. fertilization) and type (coated vs. uncoated) and subtracting out control electrode values (e.g. uncoated and uncoated probes inserted into empty seedling pods) by type, baseline environmental conditions could be filtered from the signal. A combination of looking at ΔE with respect to variable and control electrodes, and then ΔE with respect to time of those normalized electrode measurements revealed consistent signal patterns and enabled further investigation of differences in growth based on treatment (Figure 19). Further investigations in a repeated experiment using only alginate coated electrodes was able to identify a stronger change in ΔE in response to photosynthesis cycles than earlier proof of concept work (Figure 20).

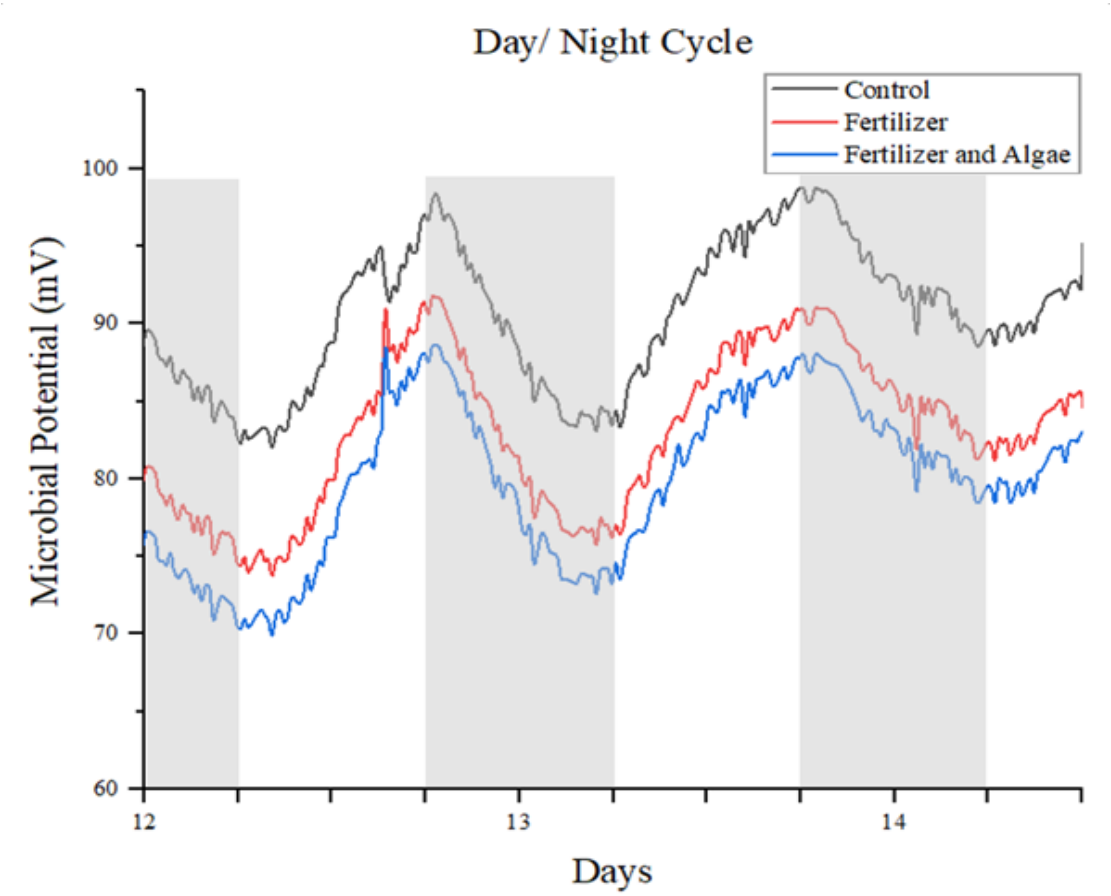

Figure 20 - Comparison of Day/Night Cycle Activity of Bonded MiProbe by Treatment Type (Qi, 2021).

Decision-Model Supported Algal Cultivation Process Enhancement Investigations

Strain Change Detection

Introduction

Microalgae cultivation is a growing industry for producing a wide variety of bioproducts from the protein and lipid content of microalgae biomass. Improving biofuels production from microalgae cultivation practices is of significant interest as a renewable alternative to fossil fuels with the added benefit of carbon sequestration. Microalgae strains of special interest in biofuels production can be morphologically similar to each other as well as less productive strains necessitating the development of tools to quickly and cost effectively characterizing cultivation productivity and quality. In some cases microalgae strain morphology can be dependent on environmental factors making consistent monitoring of microalgae cultivation unpredictable with current characterization methods. Microscopy, Optical Density, DNA analysis, flow cytometry, and MALDI-TOF (Duane Barbano, 2015) analyses offer varying degrees of confidence in characterization of microalgae strains at variable timeframes and expense. Few, if any of these analyses can provide information certainty within a work-day period and all require specialized training and significant capital expense. The MiProbe's measurement of microbial electron activity has been observed to show strong relationships with growth parameters such as biomass or nutrient loading in wastewater applications but not necessarily differentiation of dominant microbial species strains. Discerning real-time algae growth parameters using the MiProbe is of interest for improving microalgae cultivation yields and real-time detection of disruptive changes.

Real-world outdoor cultivation of microalgae strains can have substantial morphological differences from lab-grown counterparts requiring different analysis considerations to make decisions. It has been long established that *Scenedesmus obliquus*

(UTEX393) can present different morphologies under microscopy observation depending on media composition. During outdoor cultivation at the Arizona Center for Algae Technology & Innovation, UTEX393 (Figure 22) has been observed to present spherical morphologies similar to other similarly productive strains such as *chlorella vulgaris* 1201 (Figure 23). These strains are of particular interest in biofuels production as they consistently outperform other microalgae strains in Life-Cycle Analysis (LCA) and Techno-Economic Analysis (TEA) in both summer and winter cultivation conditions. The variability in cell shape of UTEX393 under industrial-scale outdoor conditions prevents using Optical Density (OD) measurements to predict current biomass production rates as measured by Ash-free Dry Weights (AFDW). The AFDW:OD ratios of consistent morphology microalgae cultures function as a reliable baseline for predicting current biomass concentrations without waiting multiple days for AFDW results to be completed using low-cost and fast OD measurements. This still requires the complexity, cost, and time investment in AFDW measurements, but allows for essential operational decision making when cultivating morphologically consistent strains.

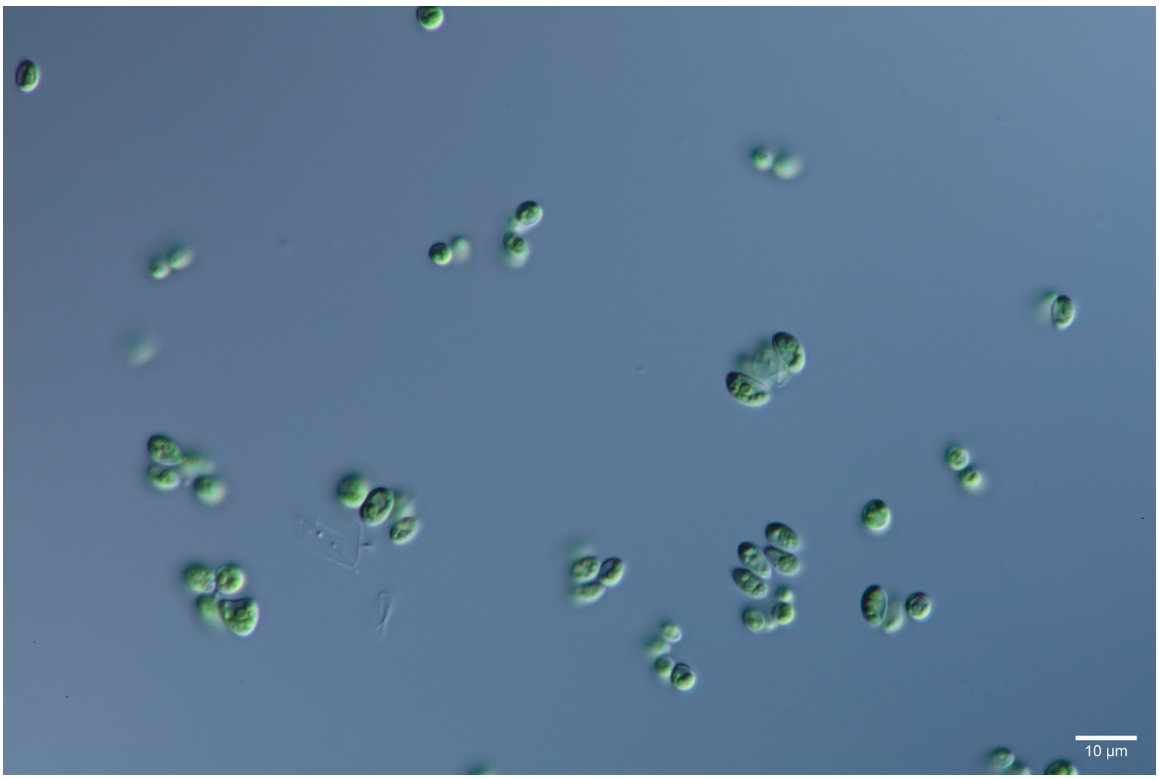

Figure 22 - Scenedesmuc obliquus (UTEX393) Seed Microscopy Showing Spherical Morphology. Credit: Aaron Geels (AzCATI, ASU).

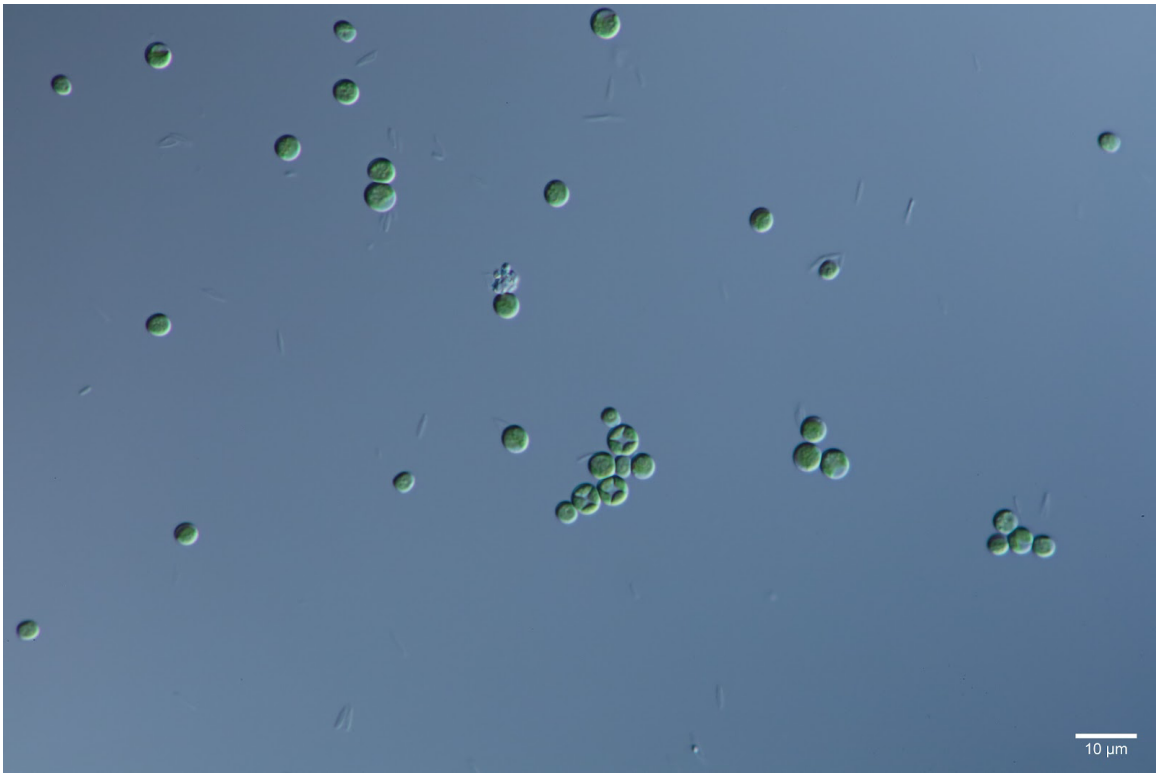

Figure 21 - Chlorella vulgaris (1201) Seed Microscopy Showing Similar Morphology. Credit: Aaron Geels (AzCATI, ASU)

Decision making for harvesting or resetting of algae ponds using current OD measurement still presents an information gap as the latest AFDW measurements are between 24 and 48 hours old under ideal circumstances and relies on high variability lab and optical measurements. If the MiProbe can accurately and continuously measure potentiometric changes in algae ponds that correlate strongly with these discrete lab sample techniques such as AFDW measurements, AFDW:OD ratios can be used less frequently to monitor quality assurance and quality control (QA/QC) parameters, reducing the need for continuous sampling, technician labor, and increase the quantity of reactor systems or volume of algae production managed by the same operations team. Furthermore, if these signal patterns can be associated with dominant cultivation strains, pond takeover events that are only detectable through more costly, technically complex, and time intensive procedures such as MALDI-TOF, Flow Cytometry, and DNA analysis, the MiProbe could dramatically reduce the costs of monitoring and improving algae production yields in homogeneous and heterogeneous bioreactor environments.

Methodology

Outdoor raceway pond cultivation was replicated under indoor controlled conditions using higher precision instrumentation and higher intensity sampling rates to confirm MiProbe biosensor behavior and its correlation with current state of the art analysis techniques. These controlled experiments were conducted to isolate changes in MiProbe biosensor signals associated with cultivation of the specific strains originally detected through intermittent PCR Analysis and eliminate any signals associated with other potential contaminants or operational characteristics.

Algae Cultivation - Outdoor Raceway Ponds

S. obliquus was cultivated outdoors in 3 replicates of 1000 L ponds with a nominal volume of 820 l, a depth of 20 cm, and a surface area of about 4.2m^2. Each pond was provided a data acquisition and control system (YSI, Inc.) measuring pH, dissolved oxygen (DO), and oxygen reduction potential (ORP), and temperature sensors, a real-time microbial sensor system (Burge Environmental, Inc.) with ORP, pH, Temperature, and 2 or more MiProbe biosensors sharing the ORP's AgCl reference electrode, a local microclimate weather station (Onset Computer Corp.) providing outdoor temperature, humidity, photosynthetically active radiation (PAR), wind speed and integrating nearby weather station API temperature, humidity, sunrise, sunset, and weather conditions (OpenWeather Project). A CO_2 sparge line was controlled with feedback provided by the control system to maintain a pH of 7 during daylight hours. A variable frequency drive was used to set paddlewheel rotation speed of 10.88 RPM continuously during both day and night cycles. BG11 standard media was used as the base nutrient media for the open raceway pond.

MiProbe biosensors were stored in chlorine water solution and cleaned between pond resets to allow the biofilm membrane to regrow after each harvest and avoid contamination risks from undesirable organisms that may have colonized the biofilm. pH and ORP probes were cleaned with chlorine and de-ionized (DI) water solutions and stored in buffer solutions between resets. Temperature and DO probes were cleaned with chlorine and DI water solutions between resets to disinfect them before redeployment. MiProbe biosensor systems were configured for 15-minute data acquisition through a cellular IoT mode of the B10 data acquisition system. The pH, ORP, and MiProbe open circuit potential measurements were configured for 250 Megaohm input impedance and +/- 2mV of precision.

Results

During normal cultivation of *S. obliquus* in outdoor raceway ponds consistent signal behavior between surface (< 5cm depth) and benthic (> 15 cm depth) MiProbes is observed after the initial biofilm stabilization period (Figure 23). Surface MiProbes have consistently stronger diurnal patterns associated with photosynthetic periods (Figure 21). Harvest periods precede drops in baseline signal and days of lower daily light intervals (DLI) decrease daily differences between daily local minima and maxima values. Despite these changes in growth and operations, rolling 2-hour variance and standard deviations show distinct ranges that are

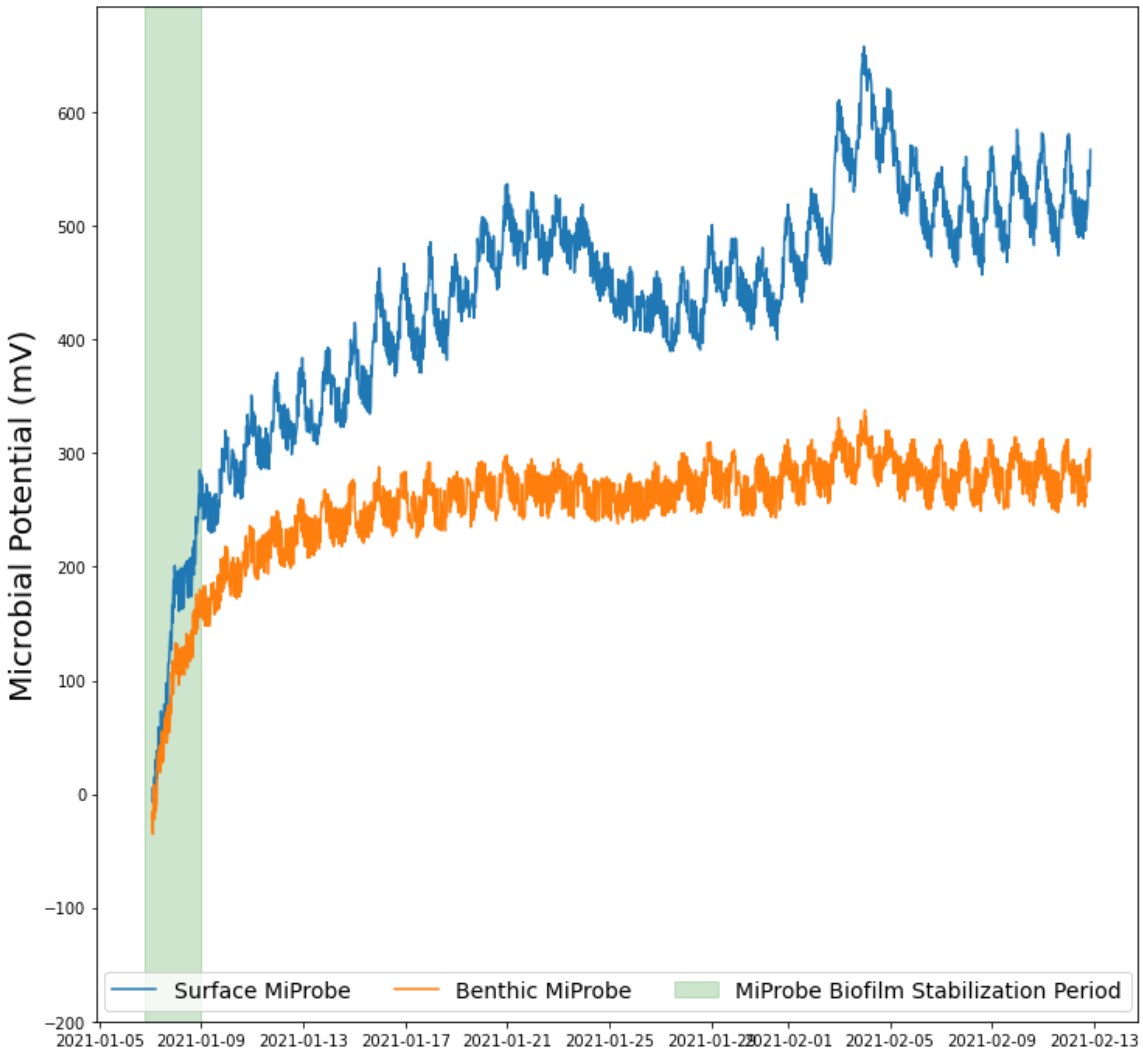

Figure 23 - Real-Time MiProbe Data During S. obliquus (UTEX393) Dominant cultivation.

consistent with dominant cultivation of a single algae strain (Figure 24, 25). These rudimentary statistical methods were investigated to provide the basis for automated alerting capabilities for further investigation of disruptions or potential crash events prior to lab analysis or visual inspection.

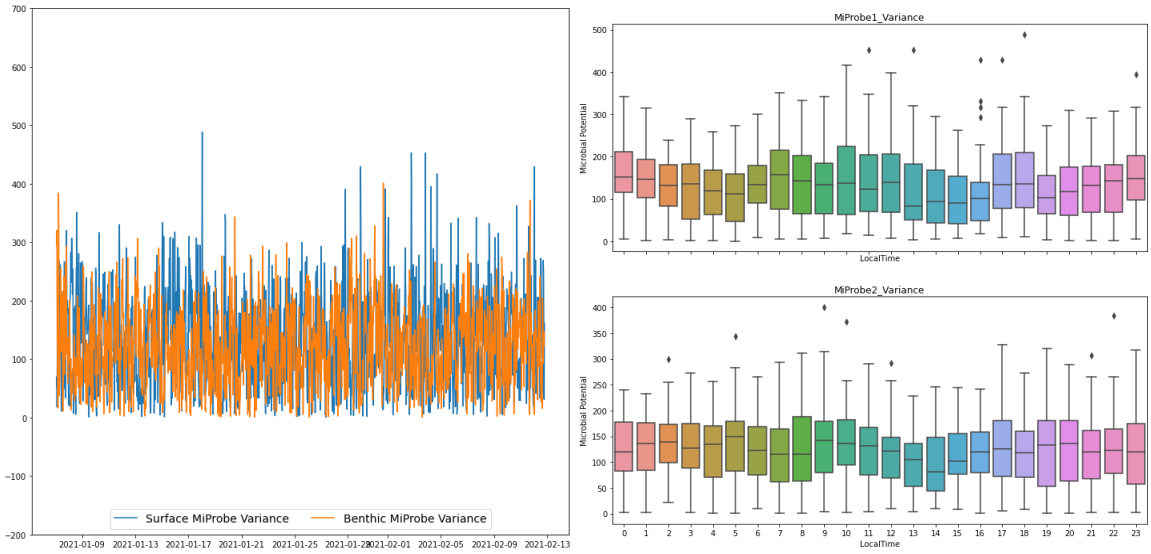

Figure 24 - Variance Analysis of S. obliquus Before Strain Change Event (Left). Surface (MiProbe1) and Benthic (MiProbe2) Hourly Distribution plot (Right).

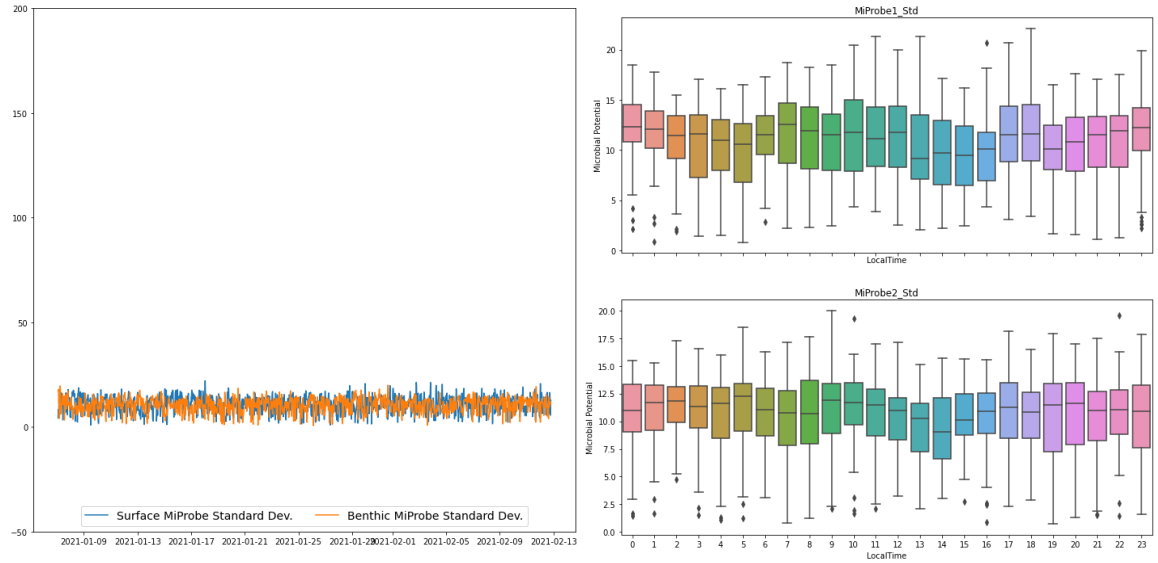

Figure 25 - Standard Deviation Analysis of S. obliquus Before Strain Change Event (Left). Surface (MiProbe1) and Benthic (MiProbe2) Hourly Distribution Plot (Right).

Strain Transition Periods

During PCR-confirmed strain-change events as reported by AzCATI's researcher Dr. Henri Gerken, distinctly different baseline, daily minima and maxima, and rolling variance and standa rd deviation values similarly shift (Figure 26, 27, 28). Microscopy confirmation of the presence of *C. vulgaris* during this period was also confirmed (Figure 29).

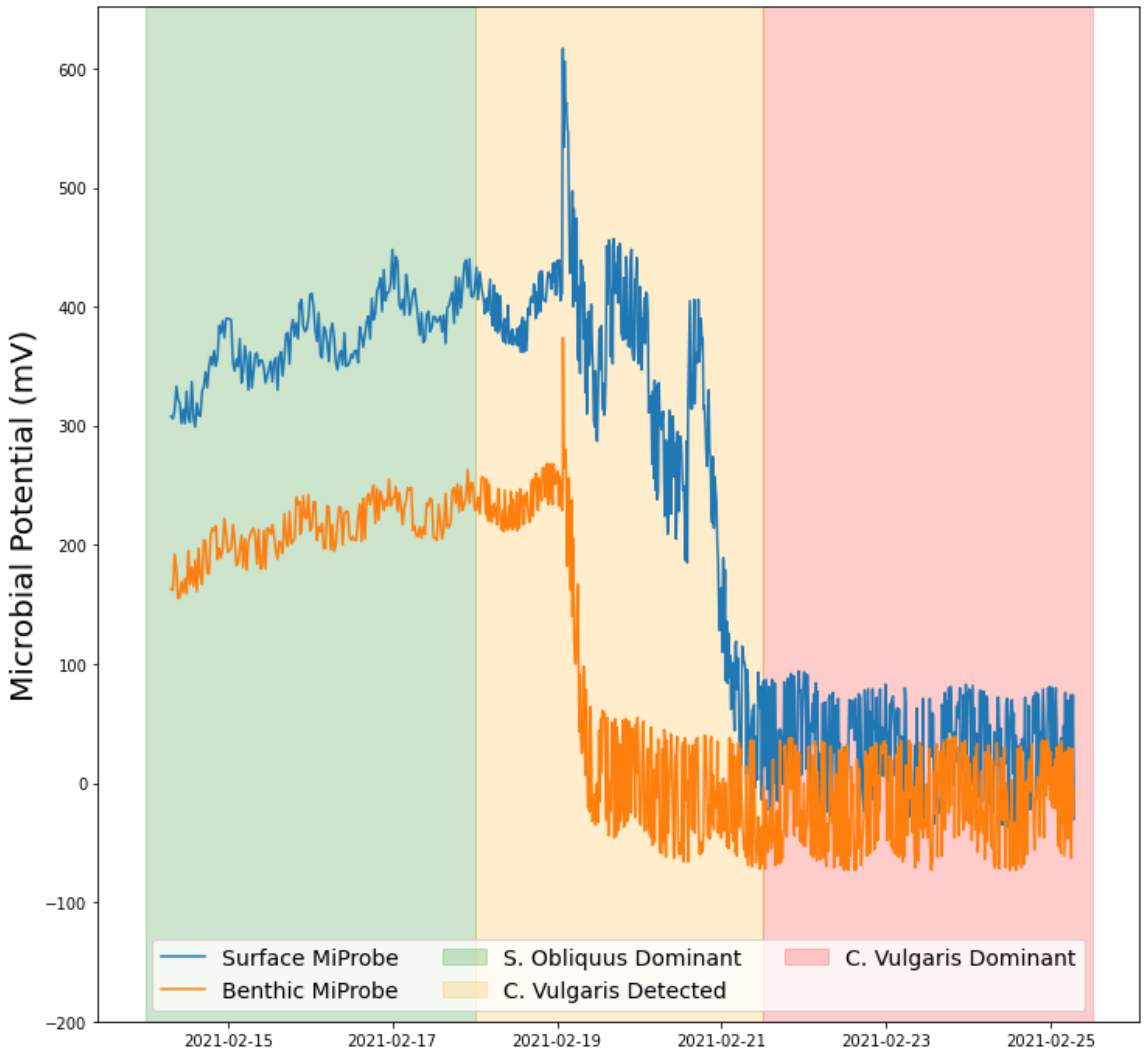

Figure 26 - Real-Time MiProbe Data Before, During, and After a Dominant Strain Change Event as Confirmed by PCR Sample Dates (Shaded Regions). PCR Analysis Credit: Henri Gerken (AzCATI, ASU)

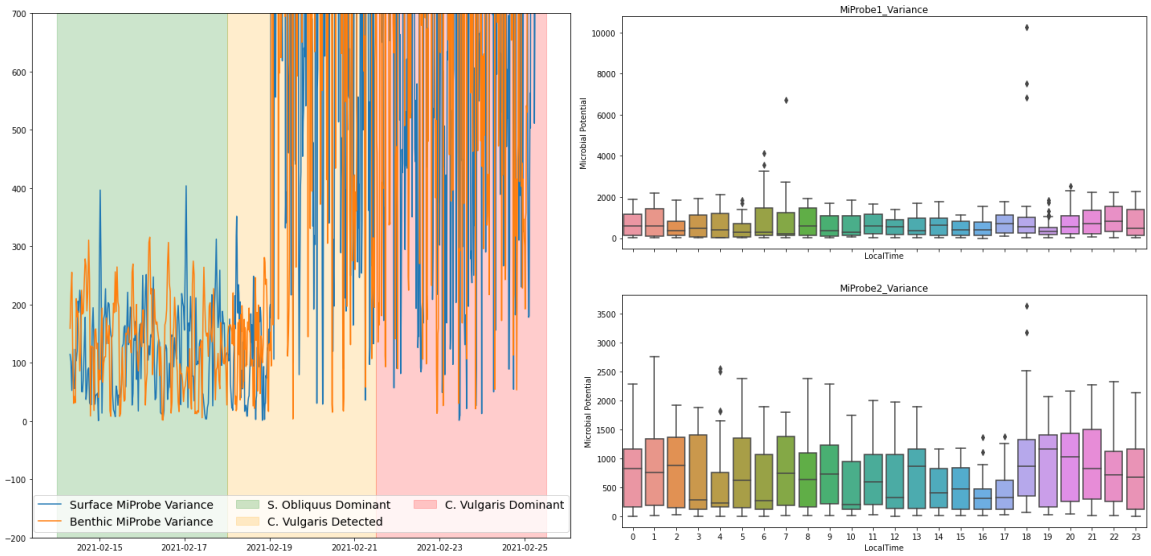

Figure 28 - Rolling Variance Analysis During Strain Change Period (Left). Hourly Distribution Plots (Right)

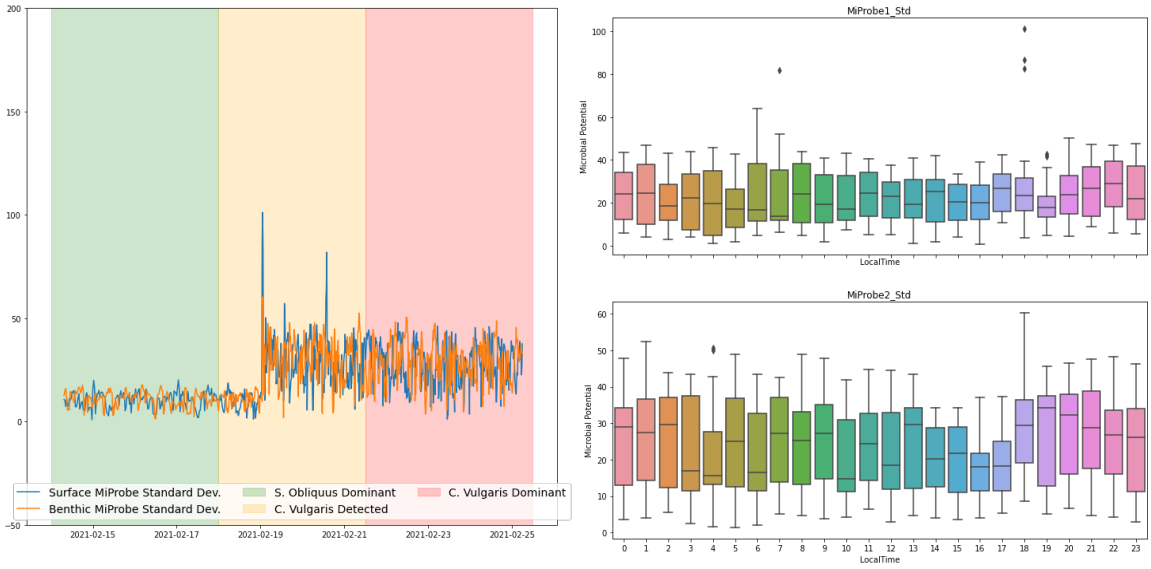

Figure 27 - Rolling Standard Deviation Analysis During Strain Change Period (Left). Hourly Distribution Plots (Right)

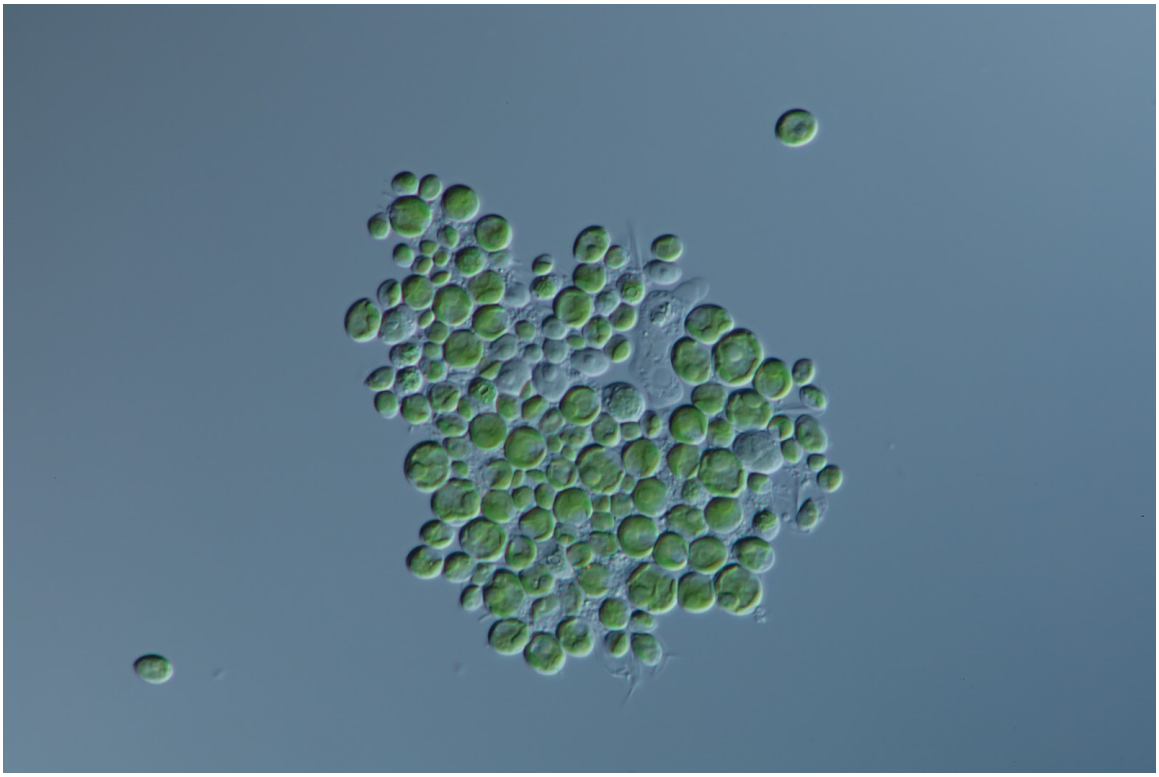

Figure 29 - C. vulgaris Detected Via Microscopy During Strain Change Event. Credit: Aaron Geels (AzCATI, ASU)

Biofilm Stabilization Period Investigations

Growth of biofilms on graphite surfaces is not an immediate process and until a stable biofilm is present, MiProbe signals may be too erratic for consistent use and interpretation (Figure 30). Electrochemical Impedance Spectroscopy (EIS) has been used to determine biofilm growth on electrode surfaces, however this method requires specialized instrumentation and expertise in interpretation and the system. In Algae raceway ponds a diurnal pattern emerges by the 2nd day of cultivation after a complete chlorination and cleaning of MiProbe sensors. Using a combination of timeseries analysis and standard box-plots give provide a way of visualizing the rolling variance of the MiProbes and quantifying raw MiProbe

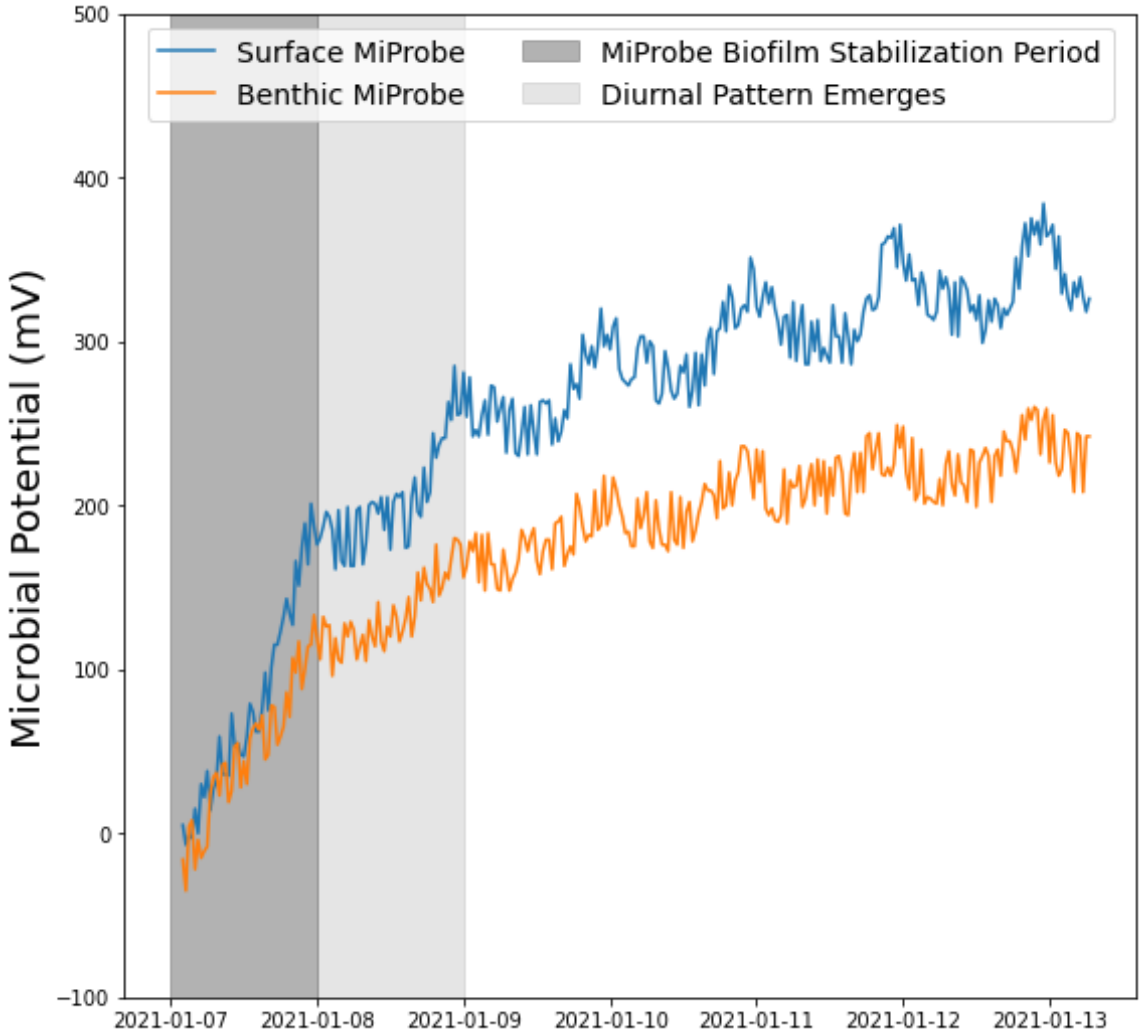

Figure 30 - Day 1-6 Real-Time MiProbe Data.

signals into a biofilm establishment or stability metric. The hourly box-plots provide insight into operationally-induced variability in signals such as 9-10 a.m. scheduled sampling and maintenance. Variability of signals during the initial deployment of probes have been an a visually identifiable indicator across pond resets, field deployments, and benchtop experimental setups.

Methods:

Hourly box plots of measurement variance distribution we plotted for both the surface and benthic MiProbes in an algae raceway basin were visualized for the first 3 days of deployment (Figures 31, 32, 33) and then from day 3 until day 6 (Figure 34). Ponds were cultivating UTEX393 as per the methodology in the later DMSCAPE investigation section of this work. Probes were prepared by cleaning off any present biofilm and storing in 5% bleach solution until reintroduced to the freshly seeded open raceway pond.

Results:

Hourly variation of measurements and boxplot distributions fluctuated substantially during the first 2 days of cultivation and probe deployment. Reduction in variance magnitude (left axis) and from day 1 to day 2 and day 3 were observed (Figures 31, 32, 33). Day 3-6 variance magnitude was consistently below 250 for all upper (e.g. 3rd) quartile box plots (Figure 34).

Conclusions:

Hourly distribution of variance may be a reliable statistical method of identifying stable biofilms on probes in algae cultivation. Evaluation of comparing both the raw MiProbe signals and decomposed variants to take into account the operational conditions of newly seeded raceway ponds may be necessary as biomass growth may a substantial part of both day 1 and day 2 variance and signal behavior.

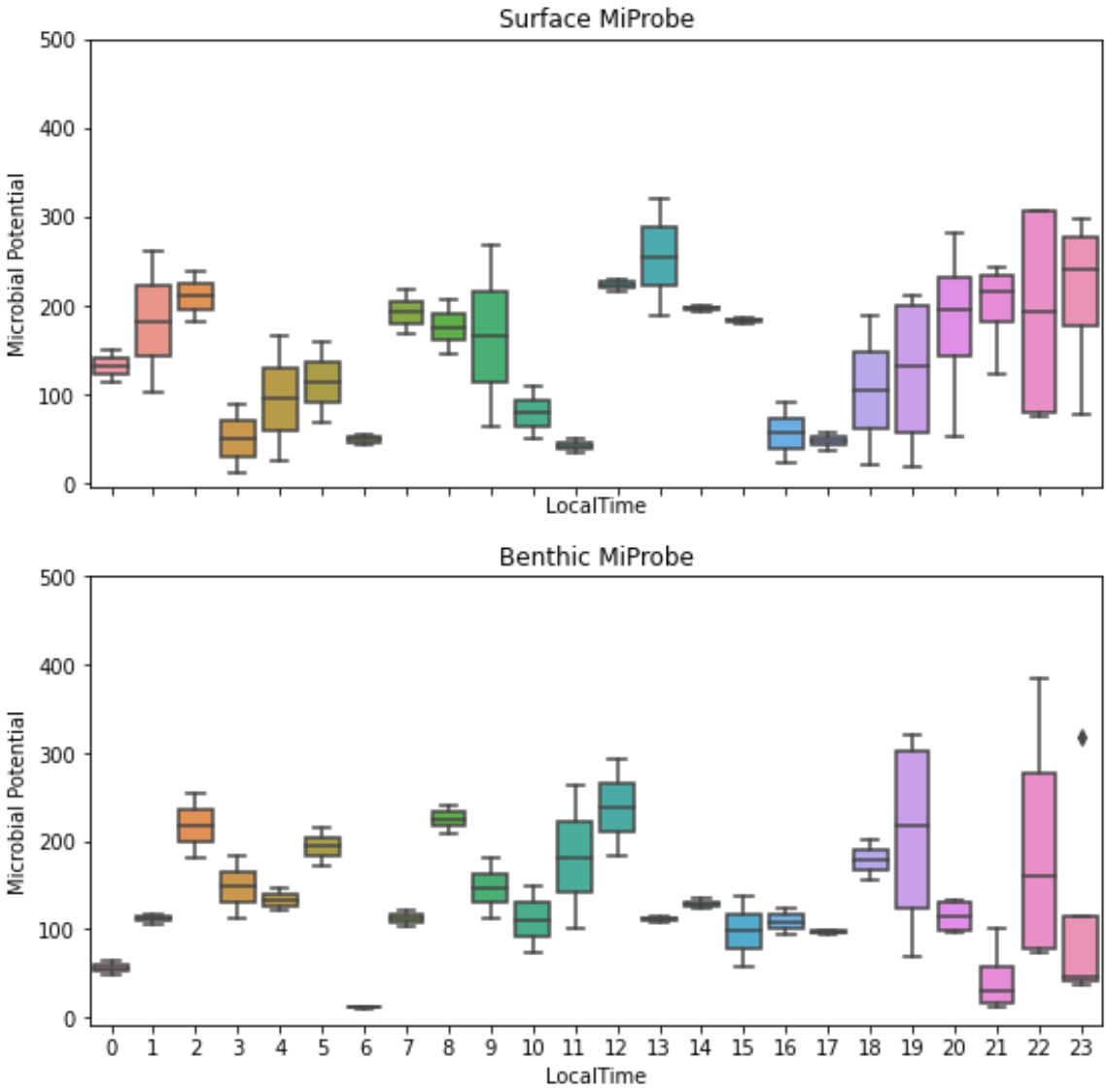

Figure 31 - Day 1 Hourly Variance Plot.

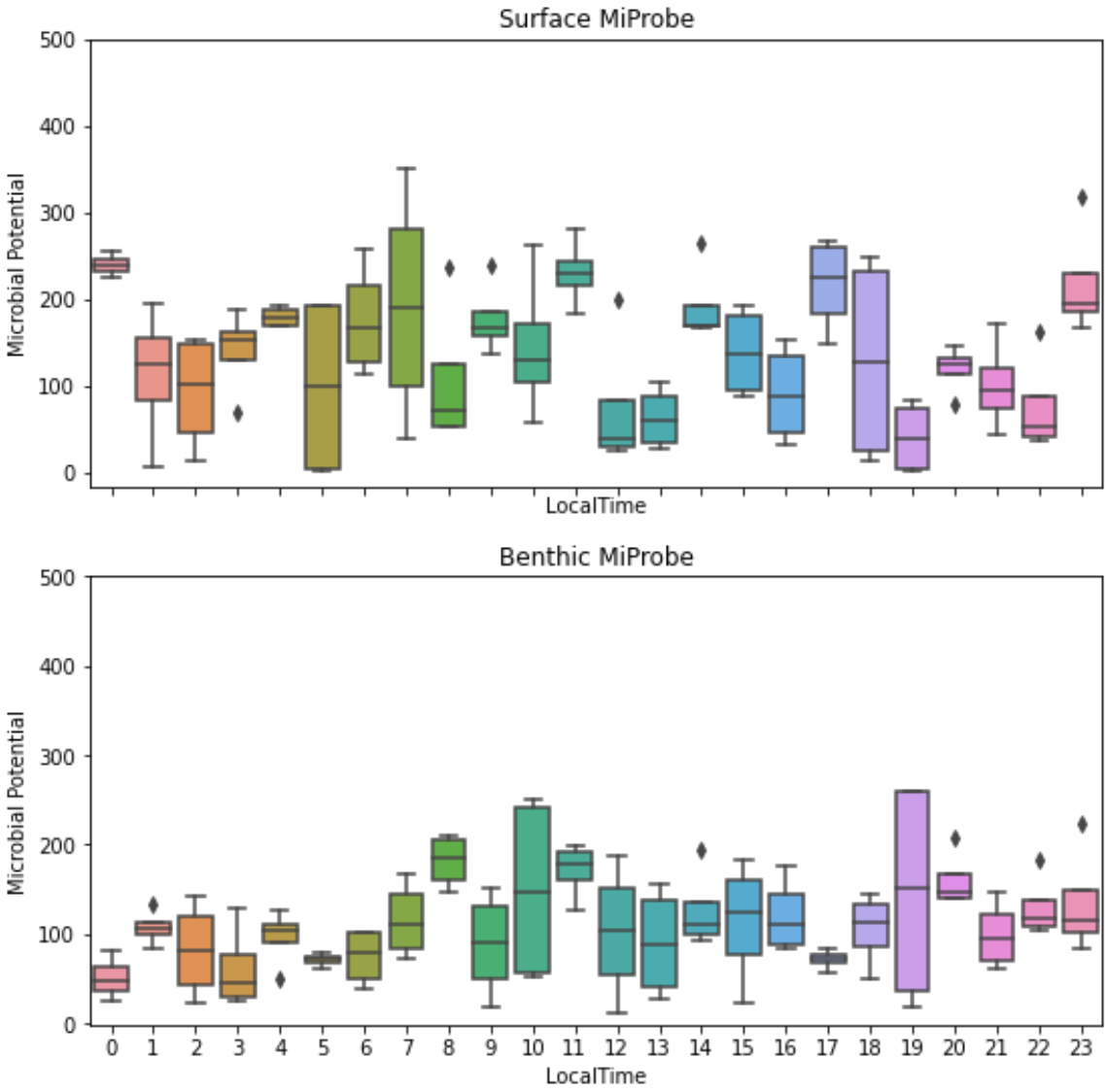

Figure 32 - Day 2 Hourly Variance Plot.

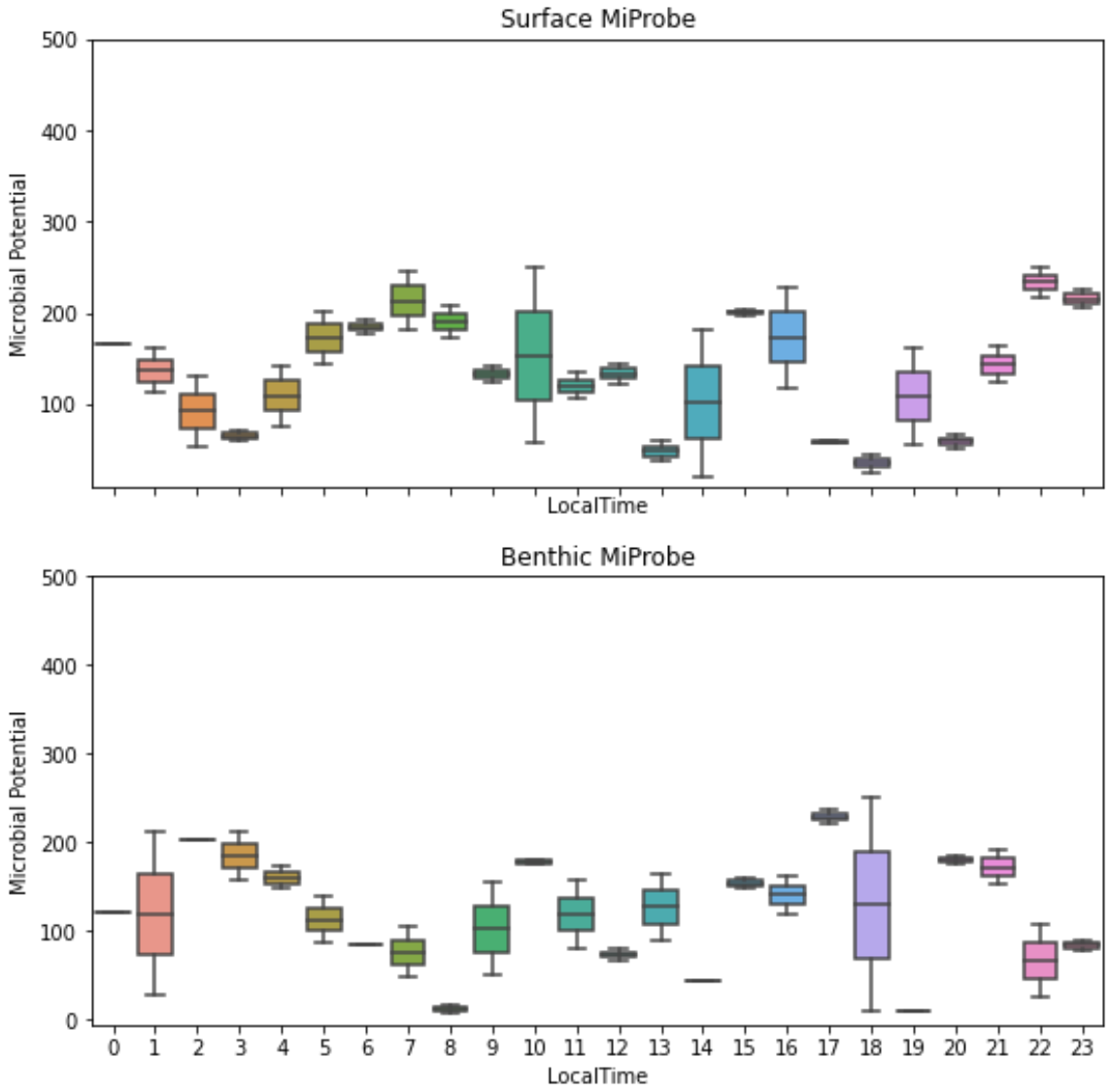

Figure 33 - Day 3 Hourly Variance Plot.

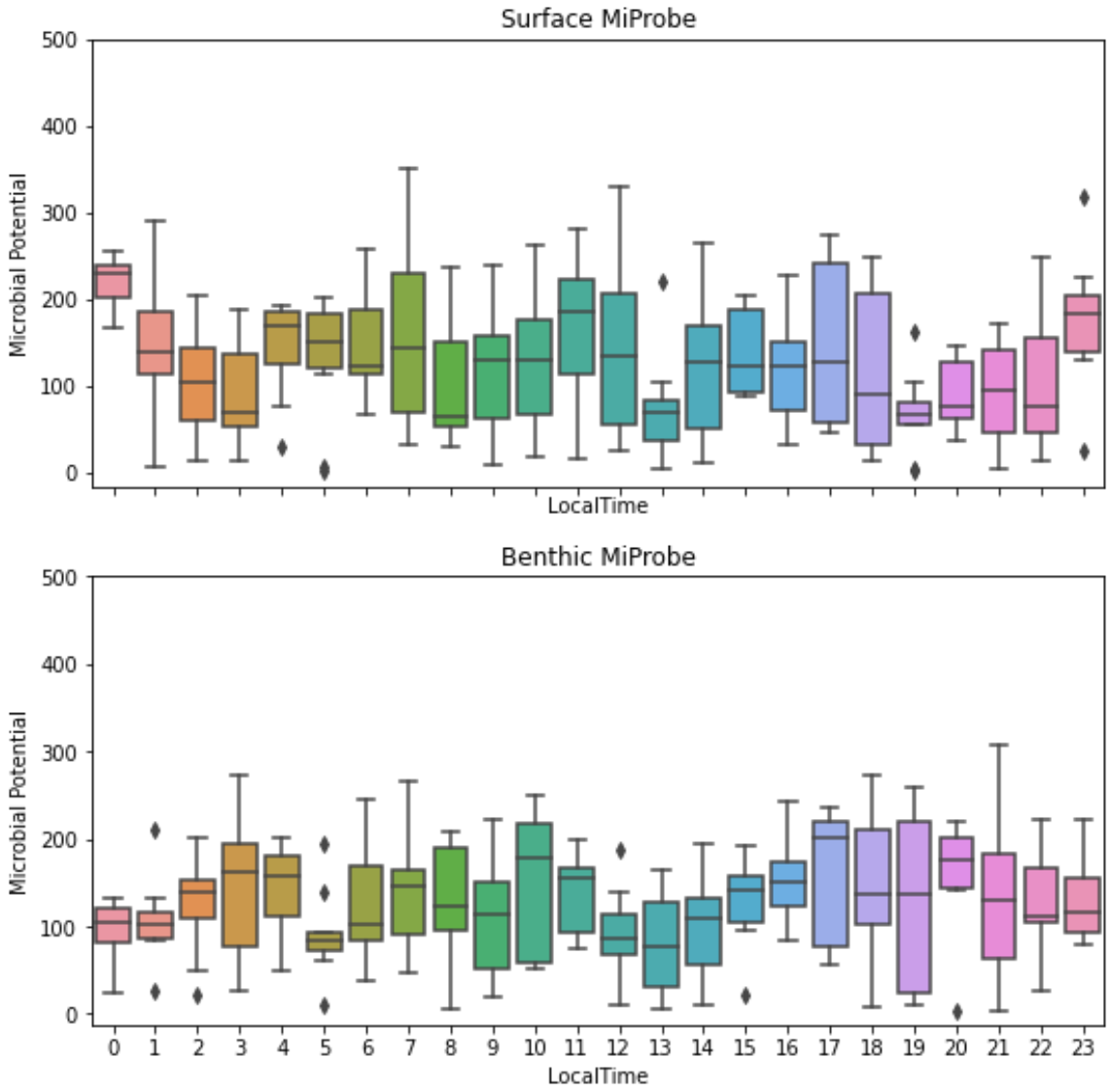

Figure 34 - Day 3-6 Hourly Variance Plot.

Alginate Hydrogel as a biofilm stabilization accelerator

Unlike wastewater bioreactor processes and environmental monitoring applications, algae cultivation is frequently done in batches from sterilized reactor conditions requiring decontamination of *in situ* sensor electrodes. Though it may only take 1-2 days to establish a biofilm membrane for MiProbe OCV measurement, this could prevent some commercial adoption if bioreactors are only operated for short time interval. Investigation into pre-coating the graphite MiProbe electrode were conducted to identify performance characteristic differences of using an alginate hydrogel as a pre-formed biofilm structure.

Methods:

Preparation of Alginate:

3.3 g of sodium alginate (Alginic acid sodium salt from brown algae, BioReagent, suitable for immobilization of microorganisms, Sigma-Aldrich) and 4.3g of MOPS were dissolved in 225 ml water. Then the suspension was stirred at 180 rpm and 95 °C until completely dissolved. The dissolved gases during the stirring process in the alginate solution were removed with a vacuum pump. Then, the alginate solution was sterilized at 121 °C for 30 min. A $CaCl_2$ solution was prepared by dissolving 2.49 g $CaCl_2$ and 4.7 g of MOPS in 225 ml DI water. The solution was autoclaved at 121 °C for 45 min.

Probe Coating Preparation:

The MiProbes were stored in 5% bleach solution and then, then washed with 30% bleach solution. The coated probes were then bonded together, by soaking in 0.1 M $CaCl_2$ solution to form the alginate hydrogel onto the graphite electrode surface. Coated MiProbe were stored in sample test tubes until redeployed in open raceway ponds.

Probe Deployment:

Both coated and uncoated MiProbes were deployed at the same depth within 5-10cm of the surface due to paddle wheel induced mixing of an established algae raceway pond. Probes were deployed 3 times over 5-7 days in ponds cultivating Phaeodactylum tricornutum (UTEX646) under the DISCOVR project. Coated probes were connected as Probe1, and uncoated probes were connected as Probe2 during the first 2 experiments, and swapped for the 3rd test. The period of investigation was from 2020-11-20 to 2021-01-11 (Figure 35).

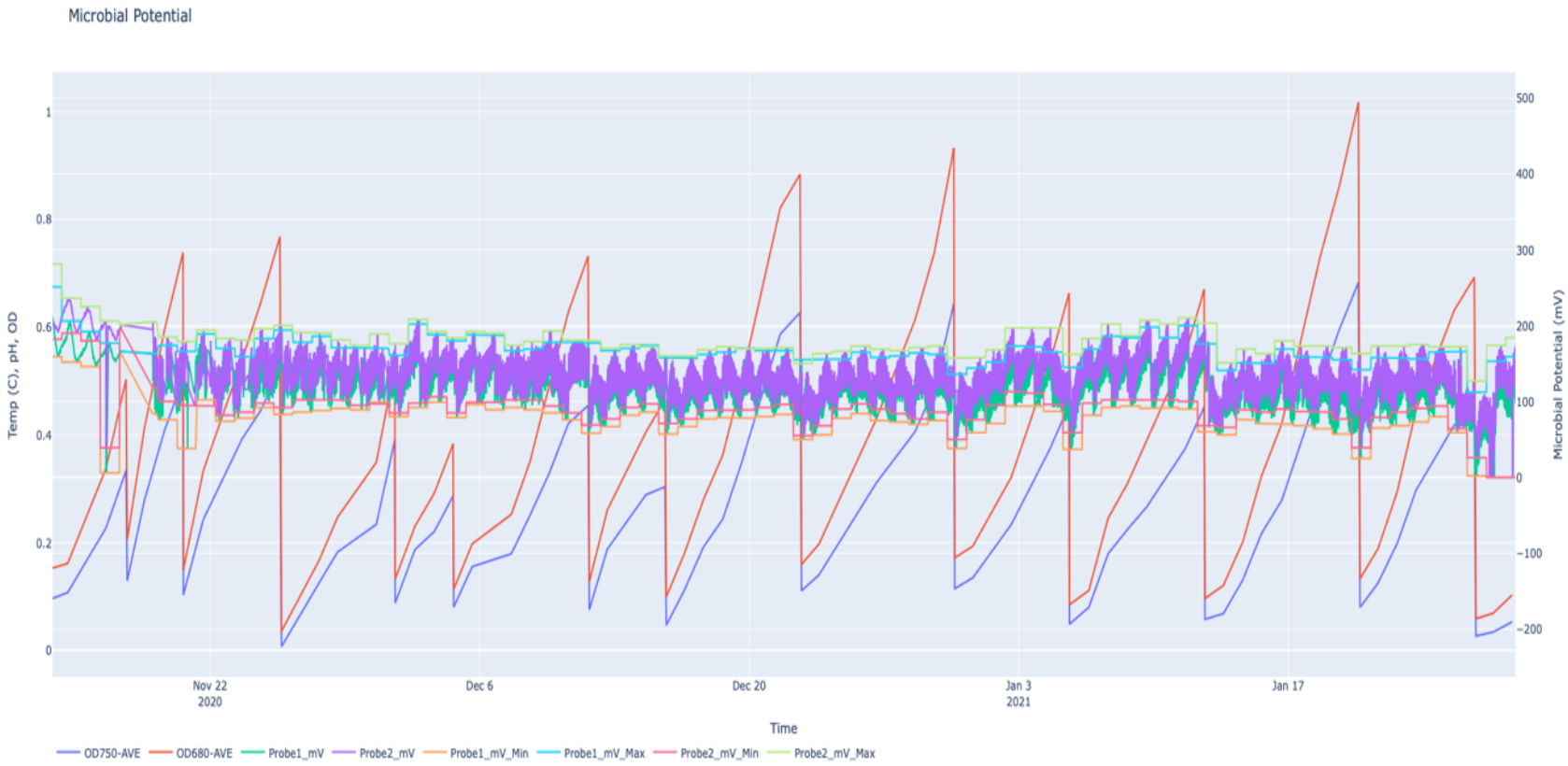

Figure 35 - Continuous Phaeodactylum triconutum Cultivation Real-Time MiProbe Sensor and Optical Density 680/750 Measurements Timeseries Data.

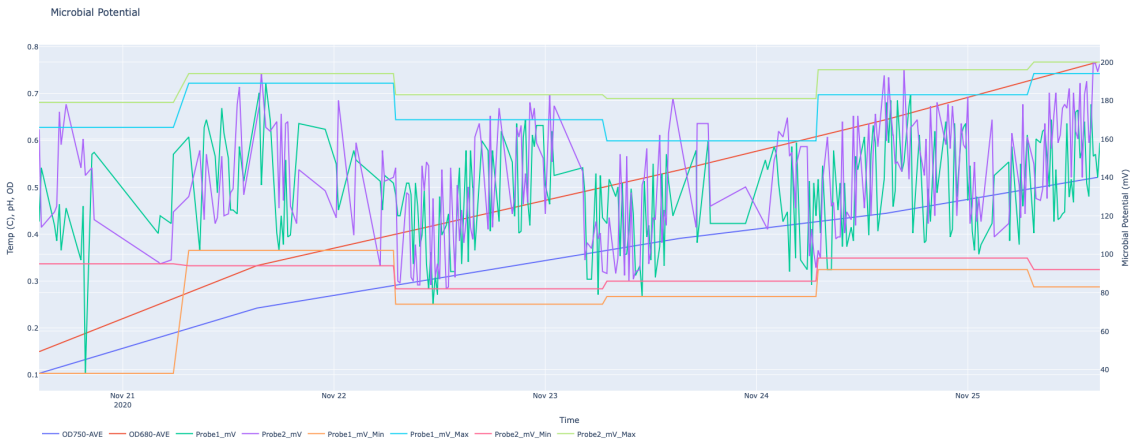

Figure 37 – Replicate 1 – Correlations of Alginate Coated and Uncoated MiProbe Daily Maxima Values Versus OD 680/750 Data.

	OD680-AVE	OD750-AVE	Probe1_mV_Max	Probe2_mV_Max
OD680-AVE	1.000000	0.997861	0.977625	0.999966
OD750-AVE	0.997861	1.000000	0.974227	0.999973
Probe1_mV_Max	0.977625	0.974227	1.000000	0.942286
Probe2_mV_Max	0.999966	0.999973	0.942286	1.000000

Table 2 – Replicate 1 -Correlation Matrix of Coated and Uncoated MiProbes Versus OD 680/750 Measurements. Probe 1 Coated, Probe2 Uncoated.

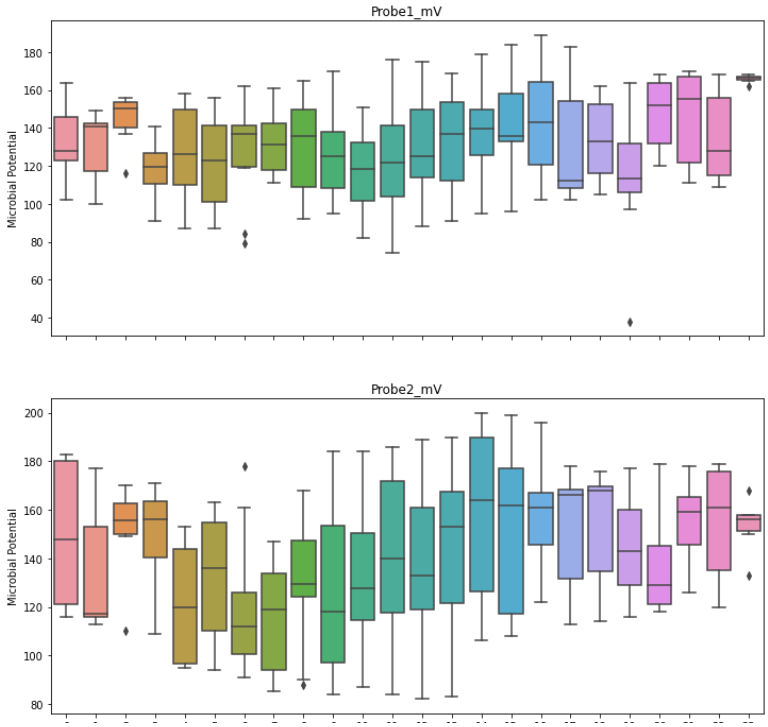

Figure 36 – Replicate 1 -Hourly Distribution Plots of coated and uncoated MiProbe variance.

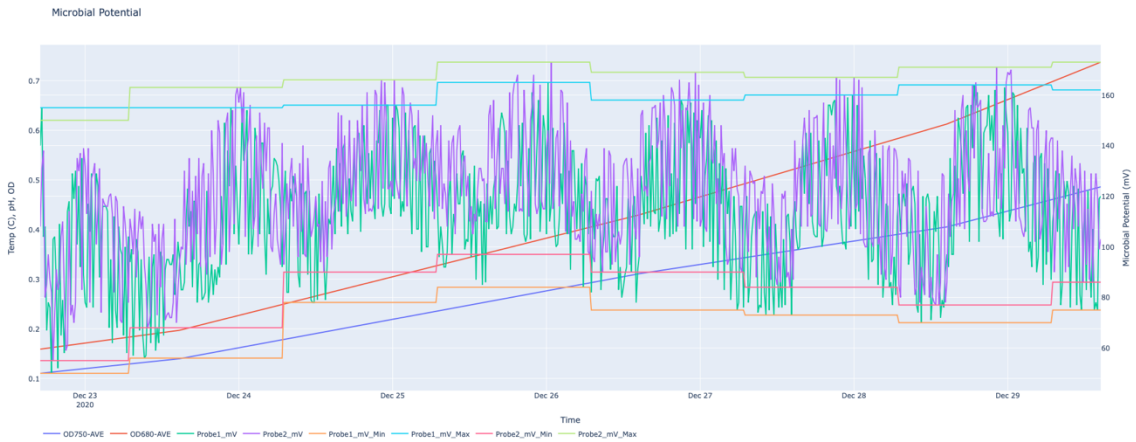

Figure 39 - Replicate 2 – Correlations of Alginate Coated and Uncoated MiProbe Daily Maxima Values Versus OD 680/750 Data.

	OD680-AVE	OD750-AVE	Probe1_mV_Max	Probe2_mV_Max
OD680-AVE	1.000000	0.997861	0.977625	0.999966
OD750-AVE	0.997861	1.000000	0.974227	0.999973
Probe1_mV_Max	0.977625	0.974227	1.000000	0.942286
Probe2_mV_Max	0.999966	0.999973	0.942286	1.000000

Table 3 - Replicate 2 -Correlation Matrix of Coated and Uncoated MiProbes versus OD 680/750 Measurements. Probe1 Coated, Probe2 Uncoated.

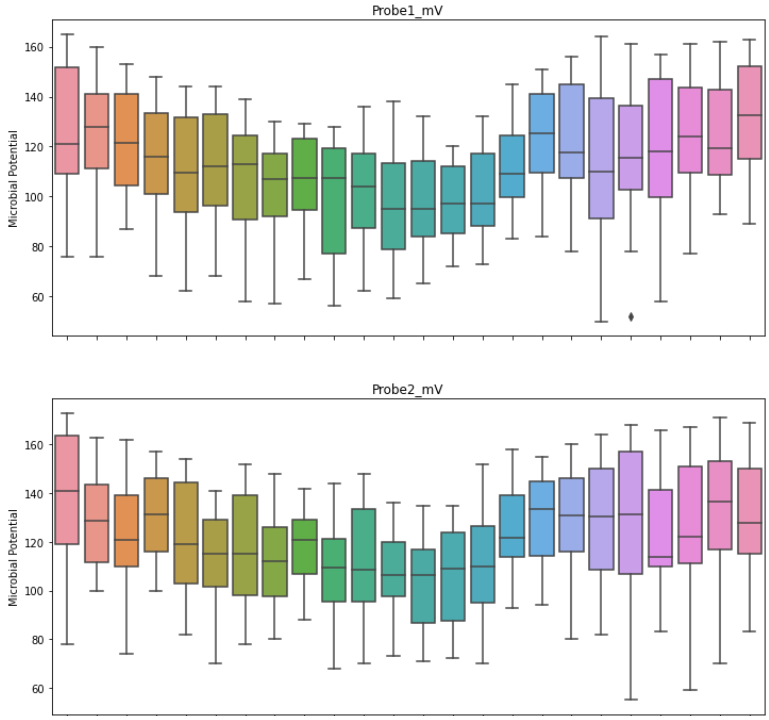

Figure 38 - Replicate 2 -Hourly Distribution Plots of coated and uncoated MiProbe variance.

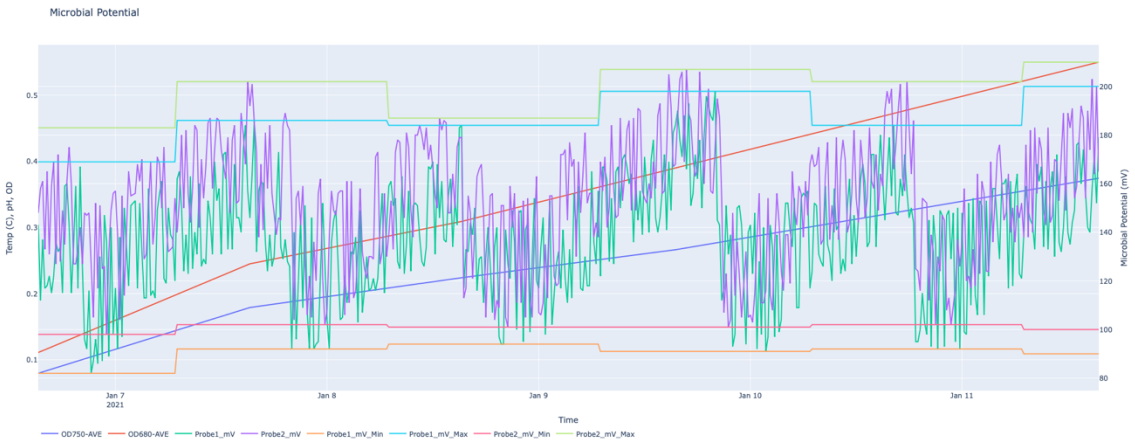

Figure 40 - Replicate 3 – Correlations of Alginate Coated and Uncoated MiProbe Daily Maxima Values Versus OD 680/750 Data.

	OD680-AVE	OD750-AVE	Probe1_mV_Max	Probe2_mV_Max
OD680-AVE	1.000000	0.998629	0.933308	0.800225
OD750-AVE	0.998629	1.000000	0.932766	0.792048
Probe1_mV_Max	0.933308	0.932766	1.000000	0.826422
Probe2_mV_Max	0.800225	0.792048	0.826422	1.000000

Table 4 - Replicate 3 - Correlation Matrix of Coated and Uncoated MiProbes Versus OD 680/750 Measurements. Probe1 Uncoated, Probe2 Coated.

Results:

No discernable difference in performance when analyzing the raw timeseries data (Figure 35), however significant drops in correlation between optical density (OD680 and OD750) measurement data provided by AzCATI (Tables 2, 3, 5, Figures 37, 39, 41). Upon further inspection, coated probes had consistently higher hourly variance of coated probes measurements were observed in each replicate in both magnitude and quartile size (Figures 36, 38).

Petri Dish Sensor Matrix

As previously demonstrated, using the experimental control electrodes as a reference to filter baseline environmental changes and amplify metabolic activity or biomass changes as a result of experimental variables, it may be possible to create a re-usable petri dish-based lab assay tool that is not reliant on conventional standard reference electrodes. Utilizing a combination of experimental methods to investigate measuring ΔE such as leaving unstreaked areas of the assay plate to function as control electrodes, or:

$$\Delta E_m = E_{variable\ electrode} - E_{control\ electrode}$$

Monitoring the data in real-time to look at changes in potential over time, or:

$$\Delta E_t = E_{electrode_{t_1}^x} - E_{electrode_{t_0}^x}$$

And visualizing the data geospatially to evaluate:

$$\Delta E_x = E_{electrode_{t_0}^x} - E_{electrode_{t_0}^y}$$

Methods:

A proof-of-concept with 55 graphite electrodes in a hexagonal grid (Figure 42) was prototyped to evaluate if differentiation of metabolic activity would be observable using experimental control-based control electrodes. The dish provided a shallow well for allowing plate medias to be poured in preparation for streaking. Plate was prepared with the standard BG11 media used in outdoor cultivation ponds at AzCATI for the *Chlorella vulgaris* quadrant

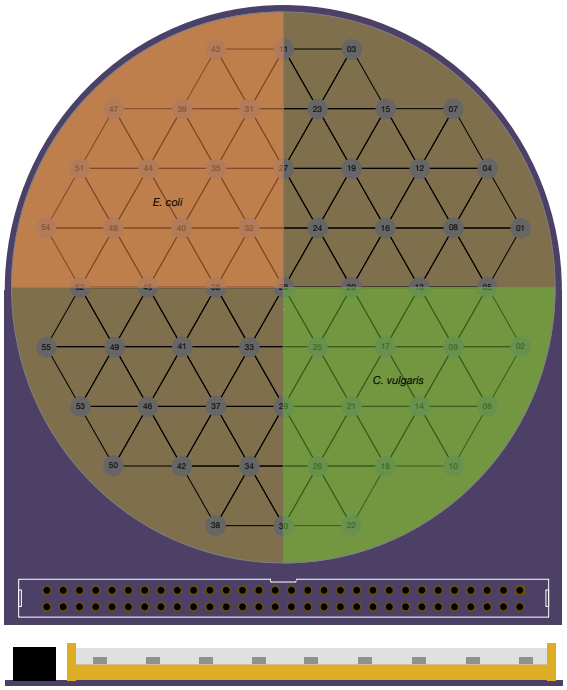

Figure 41 - Schematic of MiProbe Petri Dish with Control and Variable Streak Quadrants.

streak area but modified to provide sucrose as a feedstock for the *Escheria coli* quadrant streak. Two quadrants were left unstreaked to provide control nodes for comparing ΔE. The plate was tested in an Infors HT Multitron Shaking Incubator with a 6 hour light phase at 50% humidity, 27C, and 1.5% CO_2 followed by a 6 hour dark phase at 50% humidity, 15C, 1.5% CO_2, and a 125 rpm shaking rate. Light intensity was set to 100%/0% during light/dark phases. Data was collected in real-time at a 1-minute sampling interval by a USB-mode B56 MiProbe instrumentation board using a Raspberry Pi and the open-source miprobe python package.

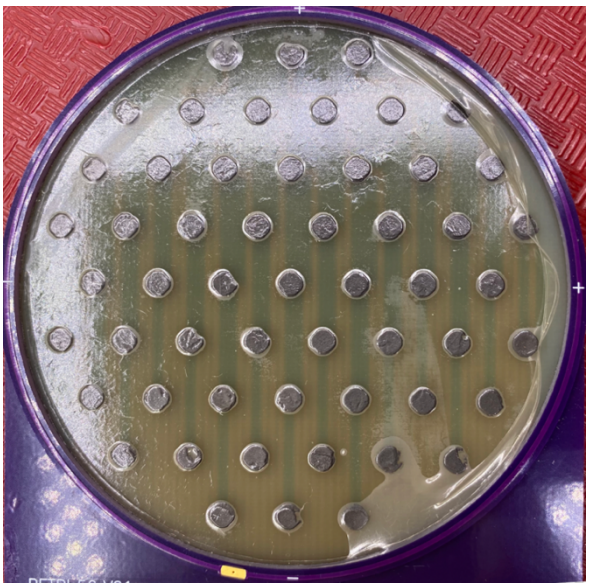

Figure 42 - Photo of Post-Experiment Peeling Due to Drying Out.

Results:

Due to a maintenance error, the incubator chamber's water reservoir emptied during the initial run of the experiment causing the modified media to peel off portions of the plate making it difficult to discern streak growth or compare electrode signals (Figure 43). While growth across the *E. coli* streak area could be observed, substantial peeling on approximately 40% of the right side of the edge of the dish, and around nearly every graphite electrode.

The experiment was repeated with an adequate water supply and monitored for 4 days. Signal patterns were distinctly different between *E. coli* and *C. vulgaris* (Figure 44, 45) and similarly to outdoor cultivation ponds, establishment and growth periods were observed over the first 24 hours before repeatable signal patterns emerged. The measurements of the unstreaked electrodes were averaged and subtracted from the variable electrodes (e.g. streaked *E. coli* and *C. vulgaris* electrode).

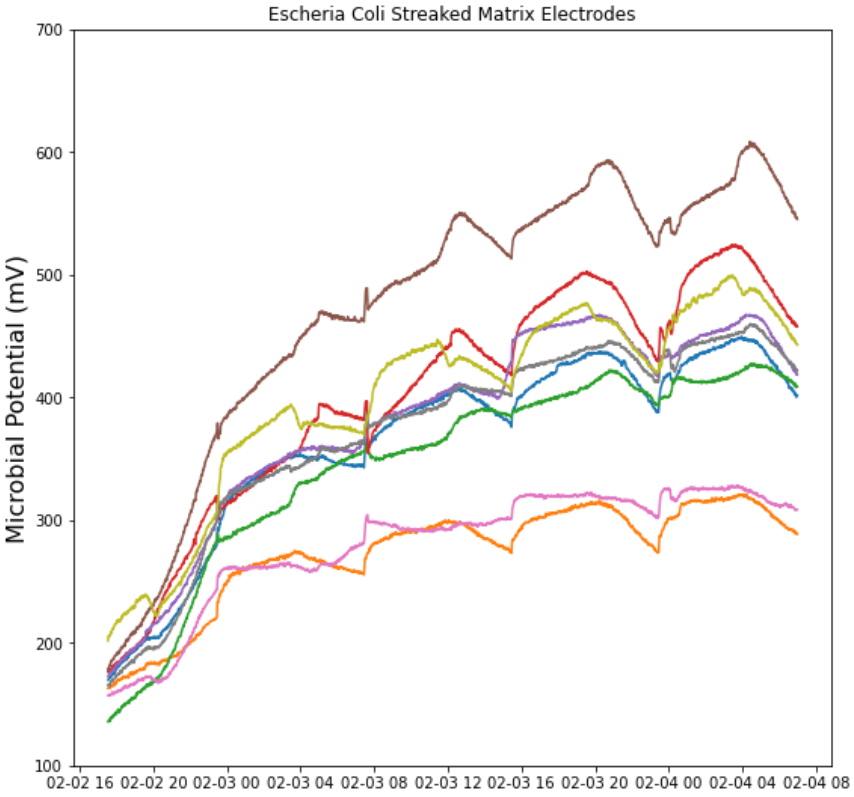

Figure 43 - E. coli Petri Dish Data from Repeated Experiment.

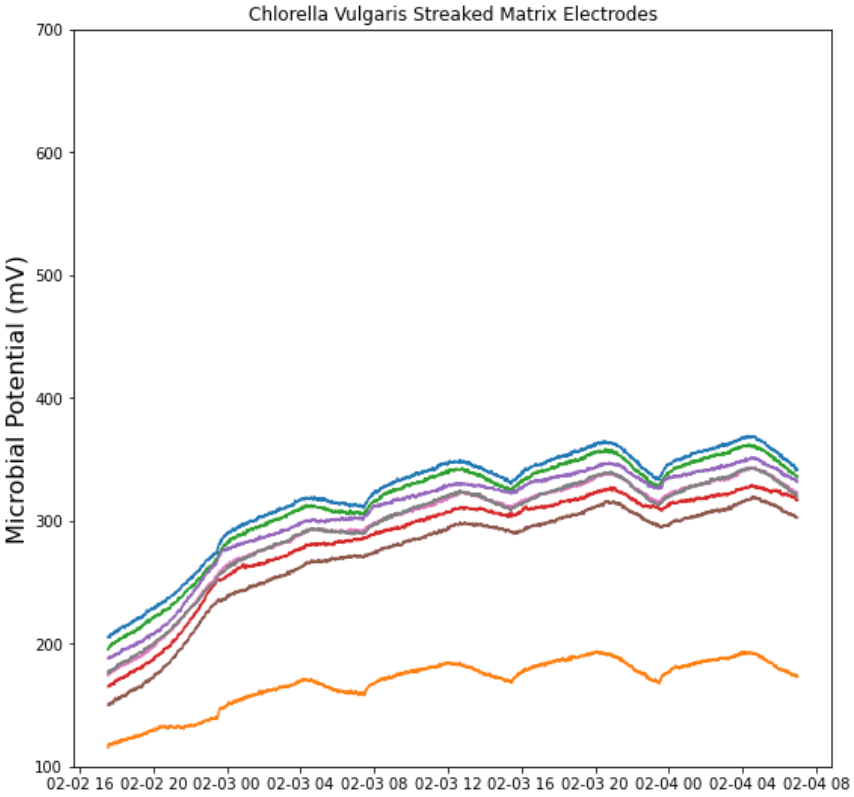

Figure 44 - C. vulgaris Petri Dish Data from Repeated Experiment.

An interactive 3D scatterplot was developed using the python package plotly to look at both the raw potential values of the electrodes (Figure 46, Top) as well as the rolling change in potentials (Figure 46, Bottom) as a tool for evaluating changes in potential with respect to geospatial and temporal considerations.

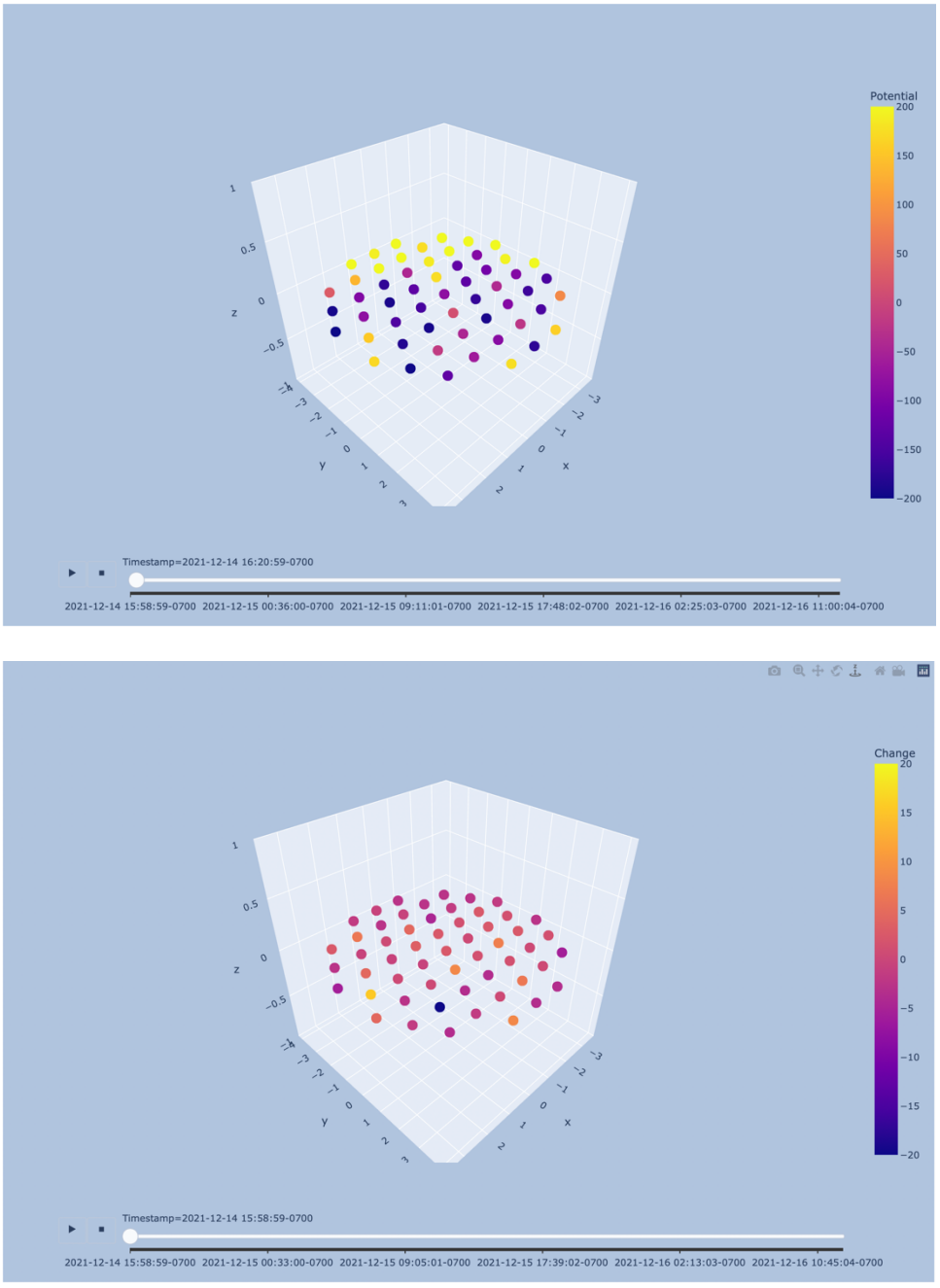

Figure 45 - Interactive 3D Visualization of Real-Time Petri Dish Data Showing Raw MiProbe Signals (Top), and Rolling Change in Potenital Over Time (Bottom).

SUMMARY CONCLUSIONS

The MiProbe may be the first of a new type of potentiometric sensor technology based on living biofilms as non-selective or partially selective membranes. This new type of sensor technology appears to generate signals associated with biological metabolic processes that can provide better information faster when coupled with real-time data analysis and visualization tools. These potentiometric signals can be decomposed and correlated with living metabolic activity directly, as opposed to potentiometric measurement of environmental variables.

This does not limit the MiProbe as the value of a real-time general health indicator that can be compared to other critical biological parameters and used for early-warning of both environmental monitoring and industrial process control disruptions. The low-cost and near-permanent lifetime of these *in situ* sensors can enable improved environmental management through reliable measurement of key ecological metabolic activity, alerting to disruptions that would otherwise require substantial capital costs and advanced expertise to monitor and analyze, and improve climate and environmental sciences through measuring the overall health of living systems in real-time.

Despite being a potentiometric measurement, the MiProbe is dissimilar from selective potentiometric sensors and cannot be evaluated using equilibrium state thermodynamic principles. The MiProbe is a living membrane sensor electrode and does not fall under any of the current Type I, II, or III Potentiometric sensor categories. The MiProbe is effectively a non-equilibrium thermodynamic state measurement tool for evaluating the change in energy in a biological system or process. As MiProbe measurements cannot be interpreted using the thermodynamically derived equations for normal types of potentiometric sensor electrodes, a

new classification of a Type IV living membrane sensor electrode is necessary to differentiate it.

Type IV sensor electrodes appear to measure the energy of the system from the perspective of the biofilm membrane. Further investigations into comparing ΔE across time, geospatially, and utilizing variable and control electrodes in experimental methodologies may reveal new understanding and be the basis for new research tools. This does not replace the use of previous types of potentiometric sensors or conventional absolute potential values, such as pH electrodes and their critical importance in understanding other potentials (Figure 1), but opens new possibilities in better understanding the biology of a system as it interacts with the chemistry of the environment.

Investigations into the use of alginate hydrogels (e.g. Agar) have revealed that in seedlings and petri dish applications the living membrane Type IV sensors can stabilize signals quickly enough to be used in rapid bioscience applications using low-cost disposable seedling electrodes and petri-dish style assays. The metabolic patterns revealed within the MiProbe potentiometric signals could have far reaching consequences in the non-destructive study of microbial and plant metabolic interactions with their environments.

FUTURE WORK

It is the Author's intention to continue investigating utilizing the principal equations for analyzing ΔE as part of a future Ph.D. program and develop improved predictive modeling for environmental applications and new analytical tools for investigating the proposed field of study of Potentiomics utilizing these Type IV living membrane sensor electrodes.

The Petri Dish application of Type IV sensors will be investigated as a new tool for ascertaining axenic culturing, isolation of both novel or genetically transformed species, and as a tool for investigating impacts of stress or therapeutic treatments on metabolic activity and function. This tool is envisioned to be able to bring down both the cost and time necessary for rudimentary to complex scientific investigation that currently requires specialized and expensive equipment and expertise.

Harmful Algae Bloom (HAB) monitoring beyond water infrastructure and into natural environments to protect critical habitat and commercial interest in fisheries is already being planned in conjunction with research centers in the Gulf of Mexico, Atlantic Ocean, and stakeholders within the Charles River Watershed in Massachusetts. This will be in addition to working with utilities such as the Central Arizona Project and the Massachusetts Water Resource Authority.

Further investigating the implications of this biosensor and more advanced analysis techniques to understand how error from applying portions of the Nernst equation variable limits (e.g. error from unknown ion concentrations z) to the real-time sensor data may reveal far greater implications of the technology for environmental monitoring than have currently been discussed. Well characterized environments or point-source polluter locations may allow real-time detection and categorization of pollutant releases as it pertains to instability or error induced from changes in ion concentration.

And most critically, developing a library of both documentation and training data on metabolic activity, abiotic disruptions, and species-specific signatures to improve AI, ML and real-time detection models to provide insights across all applications of the technology will be developed across all areas of investigation to aide researchers and practitioners in better understanding and improving processes using this new sensor technology.

The work herein will be expanded upon in collaboration with Arizona Center for Algae Technology & Innovation at Arizona State University, the Center for Contaminant Hydrology at Colorado State University, and numerous individual contributors for joint publication later this summer.

WORKS CITED

A. Bratov, N. A. (2010). Recent trends in potentiometric sensor arrays—A review. *Analytical Chimica Acta, 678*(2), 149-159.

Abe, T. a. (1996). Factors affecting selective electrocatalytic CO2 reduction with cobalt phthalocyanine incorporated in a polyvinylpyridine membrane coated on a graphite electrode. *Journal of Electroanalytical Chemistry, 412*, 125-132.

Ahmad, Z. (2006). *Chapter 2.14.6 - BENEFITS OF POURBAIX DIAGRAMS - Principles of Corrosion Engineering and Corrosion Control.* Butterworth-Heinemann.

Amini, M. K. (1999). PVC-based Mn (III) porphyrin membrane-coated graphite electrode for determination of histidine. *Analytical Chemistry, 71*(13), 2502-2505.

Anderson, O. (1927). On the logic of the decomposition of statistical series into separate components. *Journal of the Royal Statistical Society, 90*(3), 548-569.

Anne Koehler, R. D. (2001). Forecasting models and prediction intervals for the multiplicative Holt--Winters method. *International Journal of Forecasting, 17*(2), 269-286.

Bimakr, F. G. (2018). Assessing graphite and stainless-steel for electrochemical sensing of biofilm growth in chlorinated drinking water systems. *Sensors and Actuators B: Chemical, 277*, 526-534.

Chang, C.-N. a.-B. (2004). Applying the Nernst equation to simulate redox potential variations for biological nitrification and denitrification processes. *Environmental Science & Technology, 38*(6), 1807-1812.

del Olmo, D. a. (2021). Open-circuit voltage comes from non-equilibrium thermodynamics. *Journal of Non-Equilibrium Thermodynamics, 46*(1), 91-108.

Delauney, L. a. (2010). Biofouling protection for marine environmental sensors. *Ocean Science, 6*(2), 503-511.

Diana Pocaznoi, A. C. (2012). Stainless steel is a promising electrode material for anodes of microbial fuel cells. *Energy & Environmental Science*(11).

Duane Barbano, R. D. (2015). Rapid characterization of microalgae and microalgae mixtures using matrix-assisted laser desorption ionization time-of-flight mass spectrometry (MALDI-TOF MS). *PLoS One, 10*(8), e0135337.

Eric. Bakker, R. K. (1994). Selectivity of Polymer Membrane-Based Ion-Selective Electrodes: Self-Consistent Model Describing the Potentiometric Response in Mixed Ion Solutions of Different Charge. *Analytical Chemistry, 66*(19), 3021-3030.

Ganjali, M. R.-a.-R. (2001). Highly selective and sensitive copper (II) membrane coated graphite electrode based on a recently synthesized Schiff's base. *Analytica Chimica Acta, 440*(2), 81-87.

Harris, C. M. (1998). The Fourier analysis of biological transients. *Journal of neuroscience methods, 83*(1), 15-34.

Hines, W. G., & de Levie, R. (2010). The Early Development of Electronic pH Meters. *Journal of Chemical Education, 87*(11), 1143-1153.

Howard Grubb, A. M. (2001). Long lead-time forecasting of UK air passengers by Holt--Winters methods with damped trend. *International Journal of Forecasting, 17*(1), 71-82.

Huixian Ye, C. S. (2019). New alternating current noise analytics enables high discrimination in gas sensing. *Analytical Chemistry, 92*(1), 824-829.

John D. Enderle, J. D. (2012). Bioelectrical Phenomena. In J. Enderle, *Introduction to Biomedical Engineering* (pp. 648-657).

Kuhlmann, J. a. (2012). Comparison of the effects of biofouling on voltammetric and potentiometric measurements. *Electroanalysis, 24*(8), 1732-1738.

Like Gao, X. S. (2002). Continually Evaluating Similarity-Based Pattern Queries on a Streaming Timeseries. *Proceedings of the 2002 ACM SIGMOD international conference on Management of data*, (pp. 370-381).

Liljana Ferbar Trater, E. S. (2016). The comparison of Holt--Winters method and Multiple regression method: A case study. *Energy, 109*, 266-276.

Lisak, G. a. (2016). In situ potentiometry and ellipsometry: a promising tool to study biofouling of potentiometric sensors. *Analytical Chemistry, 88*(6), 3009-3014.

Meyer, H. (2021, July). Monitoring Algal Abundance, Water Quality, And Deploying Microbial Sensors Along the Central Arizona Project. Tempe, Arizona, United States of America: Arizona State University.

Partridge, H. M. (1929). A Vacuum tube potentiometer for Rapid E.M.F. measurements. *The Journal of the American Chemical Society, 51*(1), 1-7.

Philippe Esling, C. A. (2012). Time-series data mining. *ACM Computer Surveys (CSUR), 45*(1), 1-34.

Qi, D. (2021, April). The Application of a Novel Microbial Sensor on Tomato (Solanum lycopersicum L.) Growth Monitoring. Arizona, United Stated of America: Arizona State University.

Reedy, J. H. (1915). Anodic potentials of silver. *American Journal of Science*, 400-412.

Rice, D. a.-S. (96). Electrochemical self-cleaning anodic surfaces for biofouling control during water treatment. *Electrochemistry Communications, 96*, 83-87.

Rob J. Hyndman, G. A. (2018). *Forecasting: Principles and Practice.* OTexts.

Sanjay Garg, C. J. (2017). Overview of Natural Source Zone Depletion: Processes, Controlling Factors, and Composition Change. *Groundwater Monitoring & Remediation, 37*(3), 62-81.

Scott R Burge, K. D. (2020). Microbial potentiometric sensor: A new approach to longstanding challenges. *Science of the Total Environment, 742*.

Soumya Pandit, S. S. (2017). Influence of Electric Fields on Biofouling of Carbonaceous Electrodes. *Environmental Science & Technology, 51*, 10022-10030.

Tom Sale, S. G.-R. (2021). Real-time soil and groundwater monitoring via spatial and temporal resolution of biogeochemical potentials. *Journal of Hazardous Materials, 408*.

U.S. EPA (Environmental Protection Agency). (2022, 04 06). *Causal Analysis/Diagnosis Decision Information System (CADDIS): pH*. Retrieved from www.epa.gov/caddis: https://www.epa.gov/caddis-vol2/ph

Vasilis Dakos, S. R. (2012). Methods for detecting early warnings of critical transitions in time series illustrated using simulated ecological data. *PloS one, 7*(7), e41010.

Ziegler, H. (1972). A fast Fourier transform algorithm for symmetric real-valued series. *IEEE Transactions on Audio and Electroacoustics, 20*(5), 353-356.